Science of the Total Environment 846 (2022) 157479

Contents lists available at ScienceDirect

Science of the Total Environment

journal homepage: www.elsevier.com/locate/scitotenv

Application and comparison of different statistical methods for the analysis of groundwater levels over time: Response to rainfall and resource evolution in the Piedmont Plain (NW Italy)

Susanna Mancini, Elena Egidio, Domenico Antonio De Luca, Manuela Lasagna *

University of Torino, Earth Sciences Department, Via Valperga Caluso 35, 10125 Torino, Italy

HIGHLIGHTS

- Evaluation of groundwater quantitative status using different statistical methods.
- Methods: trend, change-point, percentile and non-standardized anomalies analysis.
- Comparison of the results, highlighting methods applicability and limits.
- Identification of the relations between groundwater and rainfall.
- Using more than one method is the best solution to have reliable results.

GRAPHICAL ABSTRACT

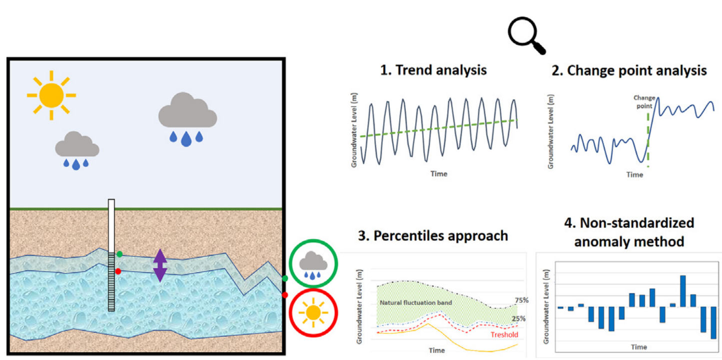

ARTICLE INFO

Editor: José Virgílio Cruz

Keywords:
Groundwater levels
Rainfall
Time series
Statistical analysis
Trends
Change points
Anomalies
Percentiles
Interannual variations
Piedmont Plain

ABSTRACT

Monitoring and analysis of groundwater level (GWL) in space and time is one of the tools used to evaluate the quantitative status of groundwater (GW) resources and identify possible alterations and critical cases due to climate change and variability, anthropogenic influences and other driving factors.

In this study, four statistical methodologies (trend, change-point, percentile and non-standardized anomaly analyses) were applied for GWL and rainfall (R) analysis in the Piedmont Plain (western Po Plain, NW Italy). To detect the interannual variations in the GW maximum annual amplitude, the coefficient of variation was also used.

The aims of the study were 1) to compare the results of different statistical methods, highlighting their applicability and differences to evaluate the quantitative evolution of GW, 2) to identify the relationship between GWL and R, 3) to investigate the spatiotemporal variation in the GWL of shallow aquifers in the Piedmont Plain, and 4) to describe critical situations of GW depletion.

The study highlights that the application of a single method for assessing the shallow GW resource status does not always guarantee a reliable evaluation. For this reason, it is advisable to apply different analysis methods at the same time. Completeness of data and medium to long time series are prerequisites for meaningful analyses. The use of the same time interval is always necessary for comparisons between different monitoring wells and between the results of different statistical analyses. Last, by spatializing the results, it was possible to identify areas characterized by similar GWL behaviour due to hydrological structure, climate variability, land use and the evolution of

Abbreviations: AN, non-standardized anomalies; ChP_GWL, change point in GWL time series; ChP_R, change point in R time series; ChPA, change point analysis; CV, coefficient of variation; CV_GWL, coefficient of variation of the maxima amplitude of annual GWL_range fluctuations; CV_R, coefficient of variation of cumulative annual rainfall; GW, groundwater; GWL, groundwater level; GWL_range, maximum amplitude of GWL annual fluctuations; GWL_AN, groundwater level anomaly; GWL_max, the highest monthly mean GWL value; GWL_min, the lowest monthly mean GWL value; GWL_T, groundwater level trend; PCTL, percentiles analysis; R, rainfall; R_AN, rainfall anomaly; R_T, rainfall trend; T, trend analysis.

* Corresponding author.
E-mail address: manuela.lasagna@unito.it (M. Lasagna).

http://dx.doi.org/10.1016/j.scitotenv.2022.157479
Received 11 March 2022; Received in revised form 13 July 2022; Accepted 14 July 2022
Available online 20 July 2022

anthropogenic activities over time. These factors influence vary locally in the Piedmont plain and require local assessments to determine the impact of changes in GWL.

1. Introduction

Groundwater (GW) constitutes the predominant reserve of fresh water on the planet and is usually large and widely distributed in the world. Groundwater contributes 42 %, 36 % and 27 % of the water used for irrigation, households and manufacturing, respectively, during 1998–2002 (Döll et al., 2012). In recent decades, GW depletion has been detected in different parts of the world (Döll and Fiedler, 2008; Wada et al., 2010) due to increasing populations, anthropic activities (e.g., overexploitation), and climate change (Taylor et al., 2013; Voss et al., 2013; Wu et al., 2020). Increasing temperature and evapotranspiration, snow cover retreat, and changing patterns and/or decreasing rainfall (R) and snow are among the major consequences attributed to climate change, and they can negatively impact GW recharge (IPCC, 2022).

The impacts of climate change on GW resources may be even more severe and amplified by intensive groundwater extraction, that represents a secondary effect of climate change itself.

Climatic and anthropogenic factors are many, impact GW resources in different ways, often overlap, and are difficult to separate (EEA, 2018). For this reason, many GW resource studies separately analyze their effects (Taylor et al., 2013; Russo and Lall, 2017).

Long-term monitoring and analysis of groundwater level (GWL) showed to be important tools for identifying possible alterations in the quantitative status and for highlighting the response of GW to climate change and the other anthropogenic global change drivers (IAH, 2016; Whittemore et al., 2016).

Statistical methods for the investigation of climatic parameters and hydrogeologically related time series are many.

Trend analysis (T) has been extensively used to assess the potential impacts of climate change and variability on natural and hydrological data, such as R, streamflow and GWL time series, in various parts of the world (Hirsch et al., 1982, Zwilling et al., 1989, Serrano et al., 1999, Zhang et al., 2001, Burn and Elnur, 2002, Arora et al., 2005, Birsan et al., 2005, Svensson et al., 2005, Abdul Aziz and Burn, 2006, Polemio and Casarano, 2008, Stahl et al., 2010, Xu et al., 2010, Zheng et al., 2010, Liu et al., 2011, Panda et al., 2012, Rusi et al., 2013, Lutz et al., 2015, Patle et al., 2015, Polemio, 2016, Amogne et al., 2018, Ducci and Polemio, 2018, Kumar et al., 2018, Pathak and Dodamani, 2019, Xia et al., 2019, Bastiancich et al., 2021). The nonparametric Mann-Kendall trend test (Mann, 1945; Kendall, 1955) and Sen's slope estimator (Sen, 1968) were applied for analyzing trends of GWL and climatic variables in different studies (Kawamura et al., 2011; Tabari et al., 2011; Krishan et al., 2015; Ribeiro et al., 2015; Lasagna et al., 2019).

Indeed, nonparametric statistical tests do not require the data to follow a particular distribution, and they are not very sensitive to the presence of possible outliers in the GWL data, compared to the parametric ones (Caloiero et al., 2011).

However, statistical analyses on time series can provide different results depending on the time period analyzed (Tomé and Miranda, 2004). Change point analysis (ChPA) can help identify abrupt changes (change points) in a time series and then split the time series into subperiods in which the parameters show homogeneous behaviors. The ChPA has been used in the field of meteorology for the analysis of changes in climate data (Lanzante, 1996; Beaulieu et al., 2012; Tirogo et al., 2016), such as air temperature, seasonal R (e.g., Tomozeiu et al., 2000; Reeves et al., 2007; Lasagna et al., 2020a), precipitation and streamflow (Kiley, 1999; Xiong and Guo, 1994), temperature (Toreti et al., 2010) and carbon dioxide concentration (Costa et al., 2016).

Other statistical analyses of fluctuations in GWL are based on the comparison of recent data with a reference value (usually a mean level) or with a range of reference oscillations (usually defined between the first and third quartile). In these cases, the considered reference values can vary the magnitude of the results (Helsel et al., 2020).

The Percentiles Method (PCTL), applied to GWL time series, is a standard groundwater evaluation tool used by the U.S. Geological Survey and proposed by the Ontario Ministry of Environment (MOE, 2008). PCTL was considered an integration of the GW drought indicator (Post, 2013). The 10th, 25th, 75th, and 90th percentiles were used to classify levels from much below normal to much above normal; in general, GWL between the 25th and 75th percentiles was considered normal, GWL between the 10th and 25th percentiles was considered dry, and GWL below the 10th or 5th percentile was considered a drought emergency.

The evaluation of standardized and non-standardized anomalies are methods widely used for the analysis of climatic variables such as R, air temperature and snowfall (Regione Piemonte, 2020; Asoka et al., 2017).

Analysis of seasonality, maximum annual amplitude of fluctuations, and interannual variability of GWL also provide additional insight into natural (e.g., climate change/variability) and anthropic (e.g., changes in irrigation practices) factors influencing the trend in GWL (Lasagna et al., 2020b). Fluctuation in the GWL occurs due to numerous factors, such as recharge (net recharge and discharge), evapotranspiration and withdrawal from wells. Its magnitude also depends on climatic factors, drainage, topography, geological and hydrogeological characteristics and anthropogenic influences (Panda et al., 2007; Krogulec et al., 2020). Sometimes high fluctuations can result in problems and undesirable effects, such as the alteration of GW flow regimes and changes in the volume and quality of available GW resources (Apaydin, 2009). Indeed, a high variability of annual average GWL fluctuations over time can lead to critical issues, such as, in the case of shallow aquifers, interference with anthropogenic infrastructures or an incorrect assessment of the GW resource, which cannot be detected through a single annual average value.

In this study, different statistical methodologies were applied for GWL and rainfall (R) analysis in the Piedmont Plain (western Po Plain, NW Italy).

A preliminary study of the hydrodynamic behaviors of the GW, their spatial distribution and R regime was conducted in this area by Lasagna et al. (2020b). Moreover, the main change drivers, especially those created by land use and climate variability in the study area, were analyzed and described.

This study represents a continuation and a deepening of Lasagna et al.'s (2020b) investigation. Starting from the current resource status, it aims to describe the most useful methods to investigate critical situations of GW depletion due to climate variability, land use and human activities. More specifically, four methods of GWL time series analysis were applied and compared: trend, change-point, percentile and non-standardized anomaly analysis. The same methodologies were applied to the R and GWL time series. Although changes in GW levels do not depend solely on climate data, comparisons and correlations between GWL and R can help to assess aquifer vulnerability to climate change (Ng et al., 2010) and to evaluate how R affects changes in the GWL. The aims of the study were: 1) to compare the results of different statistical methods, highlighting their applicability and differences; 2) to identify the relationship between GWL and R; 3) to investigate the spatiotemporal variation in the GWL of shallow aquifers in the Piedmont Plain; and 4) to describe critical situations of GW depletion. Then, the spatialization of the results of the statistical analyses and elaborations were discussed, with particular reference to geographical distribution, identifying the most critical areas.

2. Materials and methods

2.1. The study area

The study area is the Piedmont Plain (western Po Plain, NW Italy) and represents the largest and most important GW resources in the Piedmont Region.

The Piedmont Plain is characterized by different hydrogeological complexes (Fig. 1) listed from top to bottom (Bove et al., 2005; De Luca et al., 2019; Perotti et al., 2019; De Luca et al., 2020) as follows:

- Recent fluvial deposits (Upper Pleistocene-Holocene): composed of incoherent and heterometric sediments of fluvial (Holocene) and fluvioglacial (Upper Pleistocene) origin, mainly composed of gravel and sand with subordinate silty-clay intercalations; these sediments are located in the bottom of the valleys of the region and in the Piedmont Plain.
- Medio-ancient fluvial deposits (Middle-Lower Pleistocene): composed of incoherent and heterometric sediments, locally cemented, mainly gravel and sand, and silty-clay, sometimes in alternation; the fine fraction may be prevalent. These deposits, which border the Apennine-Alps chains from Tanaro River to Maggiore Lake, are in contact with the morainic arches to which they are genetically connected.
- Glacial deposits and morainic hills (Pleistocene): constituted by heterogenic glacial deposits as silt and clay with sand, cobbles and boulders.
- Lacustrine, swamp and fluvial sediments (Villafranchian series) (Upper Pliocene-Lower Pleistocene): fluvial-lacustrine deposits characterized by alternations of silty-clayey and gravelly sandy horizons.
- Marine sand and clayey silt (Pliocene): marine sediments that constitute the substratum of the Villafranchian series.

The Piedmont Plain is surrounded by the crystalline bedrocks (magmatic and metamorphic rocks) of the Alps to the N and W and by Tertiary Piedmont Basin (BTP) Hills (pre-Pliocene marine sediments characterized by conglomerate, sandy arenaceous formations and evaporitic deposits) to the S and E. A more detailed description of the geological setting with simplified cross sections can be found in De Luca et al. (2020) and in Lasagna et al. (2020b).

The shallow unconfined aquifer is hosted in the Quaternary alluvial deposits complex (Middle-Lower Pleistocene-Holocene). This complex has a thickness generally ranging between 20 and 50 m, and the hydraulic conductivity varies from high values ($K > 10^{-3}$ m/s) of recent fluvial deposits to medium ($K = 10^{-5}$–10^{-3} m/s) and low values ($K = 10^{-7}$–

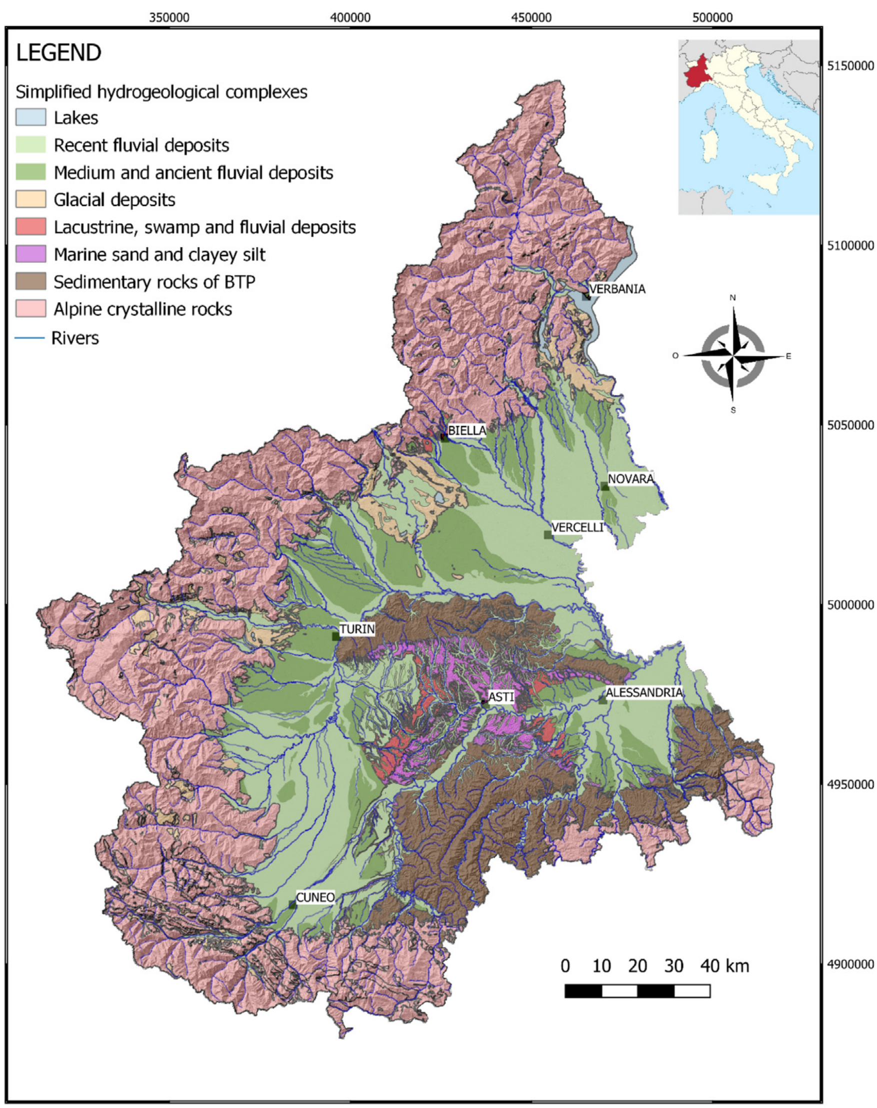

Fig. 1. Simplified hydrogeological map of the Piedmont region (NW Italy) (modified from Regione Piemonte, 2021a). Reference system: EPSG: 32632-WGS84/UTM zone 32N.

10^{-5} m/s) of medium-ancient fluvial deposits. The lower hydraulic conductivity is characteristic especially of the oldest and altered levels.

The water table depths from the ground surface are in large areas <5 m, for example, in the northern sector of the Piedmont plain (Vercelli and Novara plains), in the areas along the main watercourses (Po and Tanaro rivers) and in the plain between Turin and Cuneo. Along the band of the foothills and in particular west of Turin and southwest of Cuneo, the water table is deeper, with values generally >15–20 m from the ground surface. The highest values (>40 m) are distributed in the Cuneo Plain and in the northern part of the Turin Plain due to the presence of a high morphological terrace. In the south-eastern part of the Piedmont Plain (Alessandria Plain), the water table depths vary between 5 and 15 m from the ground surface (De Luca et al., 2020). Deep aquifers are located in the Villafranchian series and in the sandy facies of the Pliocene marine complex (Lasagna et al., 2014; Castagna et al., 2015).

In this paper, GWL analysis is conducted in an unconfined shallow aquifer characterized by medium-high hydraulic conductivity. Recharge areas of the unconfined aquifer are mainly due to infiltration of R and infiltration from the river leakage from the loosing streams in the high plain sectors. The low plain sectors are generally discharge areas, and the Po River represents the main regional discharge axis for the GW flow (Lasagna et al., 2018).

The physiographic configuration of the Piedmont region, surrounded on three sides by mountain chains and hills, favors local circulations and microclimates. The climate classification of the Piedmont Plain identifies a relatively arid central-southern area (plain of Asti and Alessandria) surrounded by a more humid area (Biancotti et al., 1998).

The analysis of the annual average temperature anomalies in the Piedmont, calculated for the period 1958–2015, shows an increasing trend over the past twenty years, with an estimated total increase of approximately 1.2 °C over 50 years (ARPA, 2010). The years after 1985 show a more marked increase in average temperature, and the increase is mainly concentrated in the winter, spring and summer months.

The average annual R from 2002 to 2017 in the Piedmont Plain was over 900 mm. During that period, 2002 was the wettest year, and 2017 was the driest (Fig. 2). The average annual R showed the lowest values (<750 mm/yr) in the SE part of the Piedmont Plain (Asti and Alessandria plain), medium values between 750 and 900 mm/yr in the central part (Cuneo and southern Turin Plains), and the highest values between 750 and 1200 mm/yr in the northern part (Novara, Vercelli and Biella Plains) (Fig. 3). The highest values of annual R were detected along the border of Plain with the mountain relief (>900 mm/yr). These values showed a similar spatial distribution detected for the period 1959–2009 (ARPA, 2010).

The annual R in the Piedmont Plain showed a seasonal behaviour characterized with a bimodal trend, with 2 maxima (spring and autumn) and 2 minima (winter and summer) typical of a continental climate (prealpine or subalpine) (Acquaotta and Fratianni, 2013; Baronetti et al., 2018).

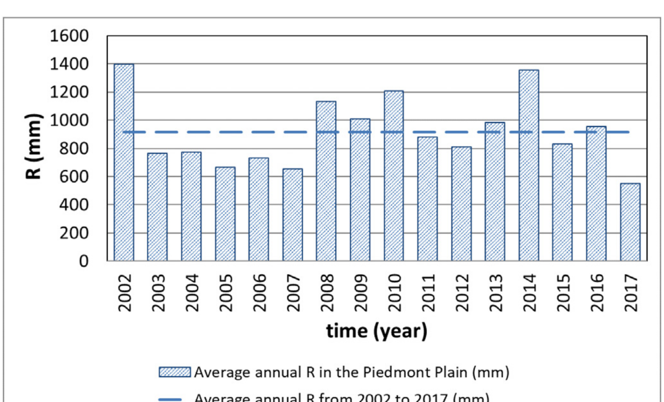

Fig. 2. Average annual R of rain gauges analyzed in the Piedmont Plain (light blue dashed line: the average annual R from 2002 to 2017).

Regarding snowfall in the Piedmont Mountains, Acquaotta et al. (2013) evaluated the annual cumulative average snowfall of the reference period 1961–2010, recorded at altitudes higher than 1000 m, varying from a minimum of approximately 300 cm to a maximum of 700 cm. 2008 was the year in which snowfall was highest, after 1950, in the last 30 years (ARPA, 2016).

2.2. Methods

2.2.1. Monitoring network and data analysis

For this study, the GWL of the shallow aquifer in 36 monitoring wells and the daily R data from 26 rain gauges distributed in the same area were analyzed (Fig. 4). The monitoring wells, homogeneously distributed in the Piedmont plain, are part of the automatic monitoring network of the Regional Agency for the Protection of the Environment (ARPA), which has been activated since 2000. Daily GWL data are available on the website of the Regione Piemonte (Regione Piemonte, 2021b).

R data are part of the automatic monitoring network Agrometeorological network (RAM) managed by Regione Piemonte, which has been activated since 2000. The R data are available on the RAM website (Regione Piemonte, 2021c).

The analysis of GWL and R time series was carried out considering a standard period of 16 years between 1 January 2002 and 31 December 2017. In this period, all the analyzed time series showed a low percentage of missing data (completeness of >90 % for GWL data and 100 % for R data). Further information about GWL and R time series are reported in Lasagna et al. (2020b).

Data were aggregated monthly, obtaining monthly averages of GWL and cumulative monthly R. Moreover, GWL was also aggregated annually.

2.2.2. Data analysis

The first elaboration in this study aimed to identify the following:

- the maximum amplitude of the GWL annual fluctuation and the average in the period 2002–2017 to quantify the annual variation in the water table in each monitoring well;
- the interannual variability in the maximum amplitude of GWL fluctuations (GWL_range) for each monitoring well in the analyzed period to distinguish wells that present a constant amplitude of fluctuation over time from those characterized by higher variability. These elaborations were conducted determining the coefficient of variation CV of annual maximum amplitude of GWL fluctuation (CV_GWL).

These parameters and their spatialization permitted to identify the areas that contain the greatest annual fluctuations and/or high interannual variability.

Different statistical methods were applied to the GWL and R time series, including a) change-point analysis (ChPA); b) trend analysis (T); c) percentile method (PCTL); and d) analysis of the non-standardized anomalies (AN). The elaborations of trends, change-points, and percentiles were performed using monthly data. Regarding the non-standardized anomalies, the analysis was performed on monthly and annually aggregated data.

Finally, comparisons were made between interannual variations, trends, change points and anomalies evaluated for R and those evaluated for GWL.

In the following, a detailed description of each adopted methodology is reported.

2.2.2.1. Interannual variability and amplitude of average annual GWL fluctuations. An accurate estimation of the spatial and temporal fluctuations in GWL and recharge is important in the management of GW resources (Rai and Singh., 1985, Cuthbert et al., 2015).

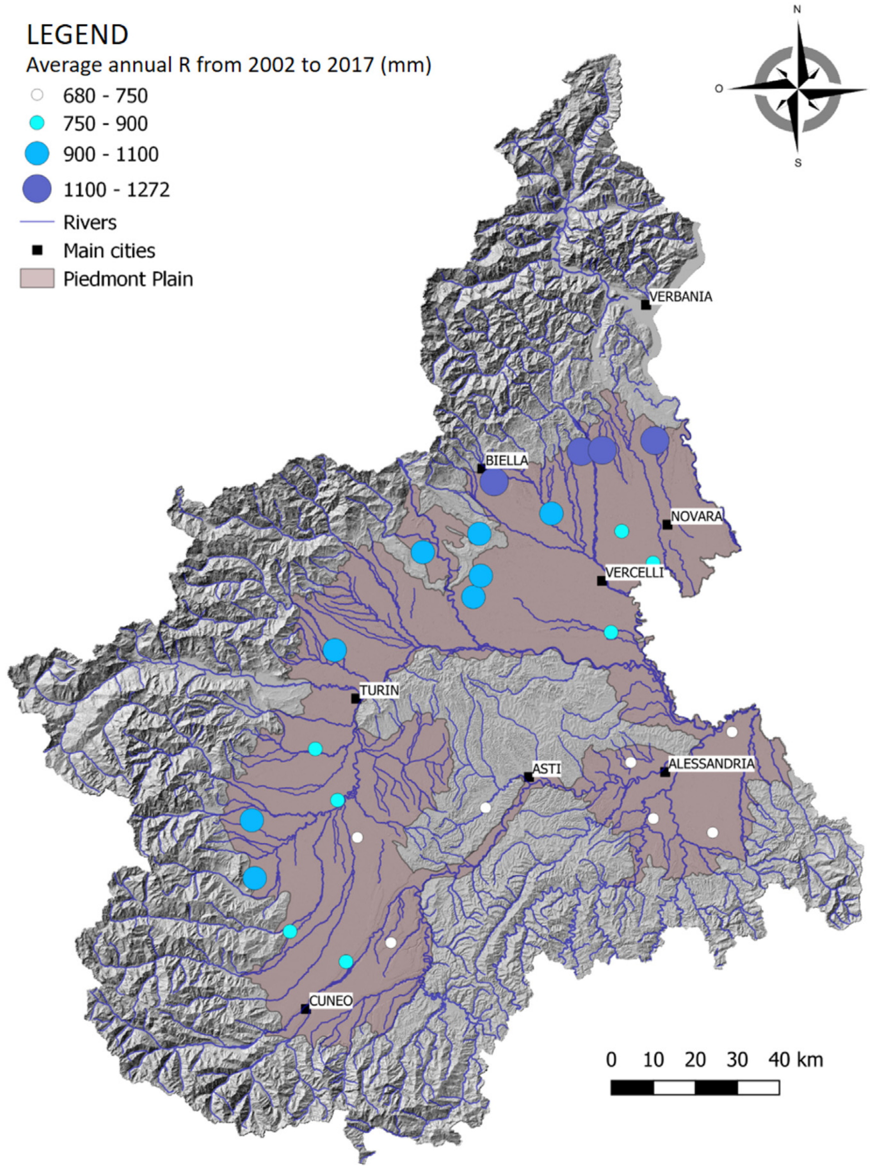

Fig. 3. Spatial distribution of annual R (average 2002–2017) in the Piedmont Plain.

For each monitoring well, the maximum amplitude of GWL annual fluctuations (GWL_range) was evaluated in the period 2002–2017. The GWL_range was calculated for each year as the difference between the highest monthly mean GWL value (GWL_max) and the lowest monthly mean GWL value (GWL_min) (Fig. S1, in supplementary materials). The maximum amplitude of annual fluctuation in GWL can vary from year to year, so for each GWL time series, the minimum and maximum values of annual GWL_range fluctuations were detected (Fig. S2, in supplementary materials) in the analyzed period.

The interannual variation of annual GWL_range fluctuations were made through the coefficient of variation (CV). The CV is independent of both unit and order of magnitude, and is defined as the dispersion (standard deviation, σ) normalized by the mean (μ) and is therefore a pure number (Soliani, 2001):

$$CV = \frac{\sigma}{\mu} \tag{1}$$

The interannual variability in the maximum amplitude of annual GWL_range fluctuations (CV_GWL) was evaluated in each monitoring well. The CV was also computed to evaluate the interannual variations in the cumulative annual R (CV_R) and compared with the CV_GWL.

Finally, the average GWL_range values, CV_GWL and CV_R were plotted on a map to evaluate their spatial distribution and the magnitude of their variability over time.

2.2.2.2. Change-point analysis. ChPA is a statistical tool for the identification of sudden changes (change points) in a time series, determining whether and when a change has taken place.

In this study, ChPA was applied to search for potential significant changes in the monthly GWL (ChP_GWL) and cumulative monthly R time series (ChP_R).

The analysis was performed by ordering the data according to time; then, the data were tested by the statistical nonparametric Pettitt test (Pettitt, 1979).

The Pettitt test is based on the values assumed by the following statistics:

$$U_{t,T} = \Sigma_{i=1}^{t} \Sigma_{j=t+1}^{T} \operatorname{sgn}\left(X_i - X_j\right) \quad t = 1 \ldots T \tag{2}$$

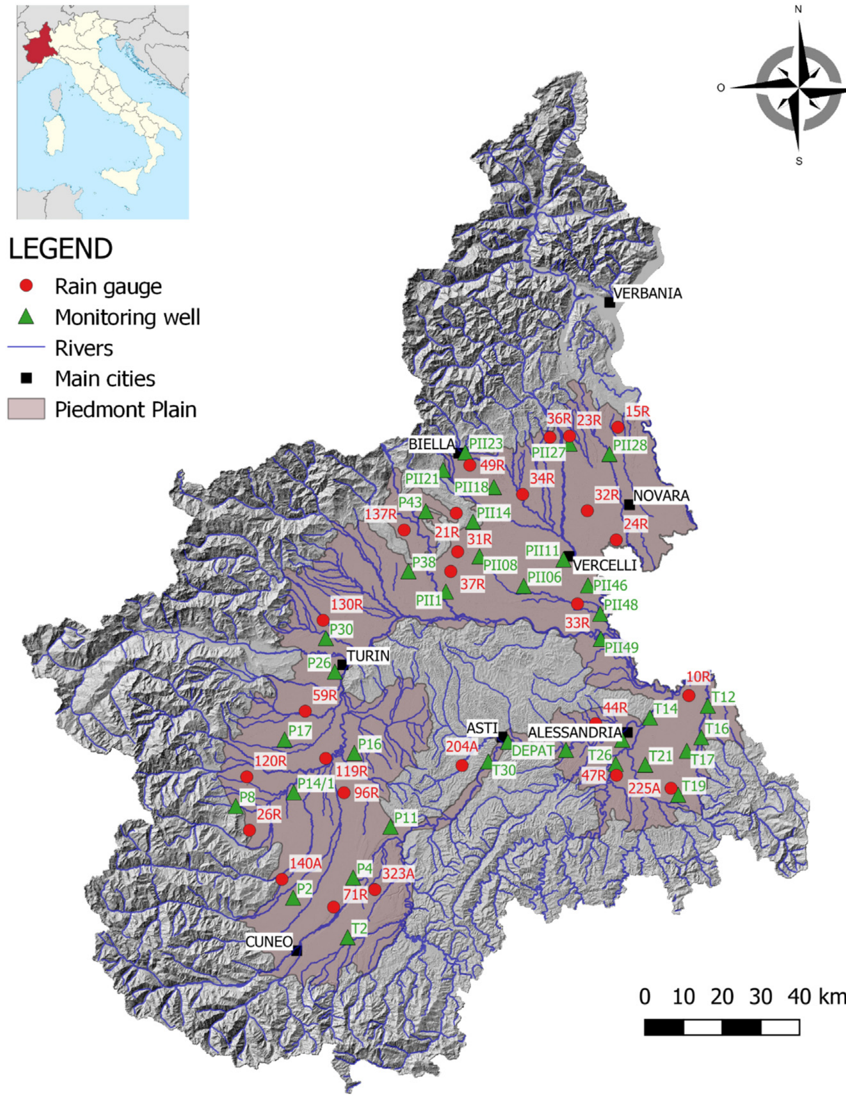

Fig. 4. Monitoring wells and rain gauges used for the study in the Piedmont Plain.

where T is the number of data in the series, X_i and X_j are data values at times i and j (with j > i), respectively, and $\mathrm{sgn}(X_i - X_j)$ is the sign function. For each value of t (instant of the series), a value of U (t, T) is obtained and plotted. The analysis of the graph of the function U (t, T) allows the identification of the moment at which a change point may have occurred. The maximum or minimum point of the function U (t, T) represents the instant in which a change point occurs if the outcome of the test were such that the null Hypothesis H_0 was rejectable at the level of significance assigned.

For this study, a 95 % confidence interval was required to state that the change was significant, with a level of significance α of 0.05.

The research and the identification of change points allowed us to obtain complementary information that could help to deepen the analysis of time series and their variability over time and the variability of all other components directly or indirectly connected (Lockwood, 2001).

A change point in a GWL time series (ChP_GWL) corresponds to a shift in the local recharge and discharge of the aquifer due to a combination of factors that can be natural (e.g., R, feeding from watercourses, snow melt, evapotranspiration due to the rise in temperature) or anthropic (e.g., massive irrigation and paddy fields, and increase/decrease in water withdrawals during the year). The characteristics of the porous media that host the aquifer can influence the delay of the response time. The ChPA was applied over the whole time series 2002–2017, and the most important ChPs for both GWL and R were identified.

Purposes of the ChPA in this work were a) to detect if there is any change in the sequence of observed time series and when it occurred; b) to estimate the number of changes and their corresponding locations in time; c) to identify the points (moments) in which to start or end the trend (Figs. S3 and S4, in supplementary materials) and to compare the temporal location of ChP_GWL with the ChP_R and determine the magnitude of delays (in months). The ChPA preceded the trend analysis to split the time series into subperiods in which the parameters show homogeneous behaviors.

The ChPA was performed using the ANABASI tool version 1.51 beta, a statistical program developed by ISPRA (Braca et al., 2013).

2.2.2.3. Trend analysis. In this study, the nonparametric Mann-Kendall test was employed to identify statistically significant positive or negative monotonic trends in the GWL (GWL_T) and R (R_T) time series, and Theil-Sens slope estimator allowed us to evaluate the magnitude of the trends.

The Mann-Kendall test statistic (S) was calculated according to:

$$S = \Sigma_{k=1}^{n-1} \Sigma_{j=k+1}^{n} \mathrm{sgn}\left(X_j - X_k\right)\ t = 1 \ldots T \tag{3}$$

$$\text{with} \quad \text{sgn}(X) = \begin{cases} 1 \text{ if } X > 0 \\ 0 \text{ if } X = 0 \text{ and } X = X_j - X_k. \\ -1 \text{ if } X < 1 \end{cases}$$

A positive value of S is an indicator of an increasing trend, and a very low negative value indicates a decreasing trend. For the Mann-Kendall test, when the null Hypothesis H_0 is rejected at the level of significance α (0.05), the data present a statistically significant trend.

If a linear trend was present in a time series, Sen's slope estimator (Qi) was used to estimate the slope (magnitude of the trend line (i.e., rate of water level decline, m/yr):

$$Qi = \frac{X_j - X_k}{j - k} \quad \text{for } i = 1, 2, 3, \ldots N \tag{4}$$

where X_j and X_k are data values at times j and k (with $j > k$), respectively. T was conducted defining a 5 % significance level, and trends were assumed to be real for p values less than this threshold (p value ≤ 0.05). The trend analysis was performed using the software ProUcl (EPA, 2016).

T was performed on the whole period between 2002 and 2017 and on two subperiods identified by the presence of a main change point in the GW and R time series. Studies applied to climate variables (Tomé and Miranda, 2004) have shown a calculation of the total linear trend as the weighted average of the partial linear trends with the identified change points as boundaries.

GWL_T and R_T were then elaborated on the entire period of the time series (2002–2017) and in shorter periods (2002–2008 and 2009–2017), delimited by the presence of a main change point in the year 2008 (Figs. S3 and S4, in Supplementary materials). Finally, the spatial distributions of the GWL and R trends were mapped.

2.2.2.4. Percentiles method. PCTL allowed us to identify, for each measurement station, a threshold limit of GWL below which the GW resource starts to show issues.

The PCTL method, proposed by ISPRA (ISPRA, 2017), is based on the measure of the "natural fluctuation band" obtained by interpolating the monthly values of the 25th and 75th percentiles computed in the time interval 2002–2015 (Fig. S5, in supplementary materials).

GWL below the range of natural oscillation of GWL (less than 25th percentile) places the aquifer body in a condition of 'Alert' from the point of view of the quantitative status. Values of GWL below 15–30 % of the natural annual oscillation band are considered critical conditions for the quantitative status of water body monitoring.

In this study, threshold values were set to 15 % of the natural fluctuation band below the 25th percentile of GWL (GWL_threshold of Fig. S5, in Supplementary materials).

Finally, a spatial distribution of the number of months (for the year 2017 as an example of the method application) below or above the defined threshold was performed.

2.2.2.5. Non-standardized anomalies. A climatic anomaly is calculated from the difference between the annual (or monthly) values (X) of the hydrological variable (e.g., R) and the average values of the reference period (μX_{ref}) of the hydrological variable considered:

$$AN = X - \mu X_{ref} \tag{5}$$

According to the World Meteorological Organization (WMO, 2017), the reference period to detect the level of anomaly of the analyzed variable should be at least 30 years (i.e., 1961–1990, 1991–2020). However, it was found that 10–12 years of data provided a predictive skill similar to that from a standard 30-year period. While such short periods cannot be considered to be climatological typical standards or references, they are still useful to many users, and in many cases, there will be benefits to calculate such averages operationally (WMO, 2007).

The non-standardized anomaly (AN) method was applied to the annual GWL and R data. The reference values (GWLref and Rref) were computed considering the average values of the period 2002–2015. (Fig. S6, in Supplementary materials).

A negative anomaly indicates that the observed GWL was lower than the reference value, while a positive anomaly indicates that the observed GWL was higher than the reference value. Finally, a spatial distribution of the positive and negative annual anomaly values for 2017 was performed.

3. Results

3.1. Interannual variability and amplitude of average annual GWL fluctuations

From 2002 to 2017, the average GWL_range fluctuations in the Piedmont Plain varied between 0.37 m (monitoring well PII21) and 4.58 m (T17) (Table 1 in Supplementary materials). The minimum annual GWL_range fluctuation was 0.19 m (P43 in 2007), whereas the maximum value was 7.48 m (T17 in 2015).

Most of the monitoring wells showed an average of the maximum amplitude of GWL annual fluctuations lower than 2 m. More specifically, 36 % of the monitoring wells had an average GWL_range lower than 1 m, and 44 % had an average GWL_range between 1 and 2 m. Only 11 % of the monitoring wells showed an average GWL_range between 2 and 3 m, and the remaining 9 % had values higher than 3 m (Fig. 5).

Monitoring wells located in the Cuneo Plain, in the southern part of the Turin Plain and at the base of the mountain reliefs showed an average GWL_range lower than 2 m. Average GWL_range values higher than 2 m were found in monitoring wells located in the Alessandria Plain and along the western edge of the paddy field area in the Vercelli Plain.

The CV allowed us to measure the relative variability of interannual GWL_ranges and thus to compare groups of data according to their degree of variability. In the study area, the CV of the annual GWL_ranges (CV_GWL), evaluated for each GW time series, varied from a minimum of 0.11 to a maximum of 0.47. The CV_GWL allows separating the GWL time series into 3 different groups (Table 1, in Supplementary materials).

The highest interannual variations in the GWL (observed in 25 % of the total wells) were located in the Alessandria Plain (CV_GWL > 0.40). The lowest variations (22 % of the total wells) were located in the paddy field area (Vercelli and Novara plains CV_GWL < 0.20). In the other areas of the Piedmont plain (the remaining 53 % of wells), the CV has intermediate values (0.20 < CV_GWL < 0.40) (Fig. 6).

The interannual variation of R in the period 2002–2017 (CV_R) showed, in some areas, lower values compared to those of GWL amplitudes (Table 2, in Supplementary materials). The interannual variation in R in the Piedmont Plain identified a CV_R that varied between 0.22 and 0.37. Twelve percent of the annual R time series showed an interannual variation lower than 0.25 (CV_R < 0.25), 38 % showed CV_R values between 0.25 and 0.30 (0.25 < CV_R < 0.30), and 50 % showed CV_R values higher than 0.30 (CV_R > 0.30) with a maximum value of 0.37. These values are in accordance with the global values observed by Fatichi et al. (2012), ranging between 0.15 and 0.5 in approximately 92 % of worldwide rain gauges.

The spatial distribution of CV_R showed that the areas with high variation were located in the Alessandria and Cuneo plains and partially in the Novara and Vercelli plains (with CV_R ≥ 0.30–0.37). A medium variability of annual R was located along the border with the mountains and in the Turin Plain (with CV_R ≥ 0.22–0.30) (Fig. 7).

3.2. Change point analysis

The GWL and R data from 2002 to 2017 were analyzed to identify ChP_GWL and ChP_R in the time series.

Three statistically significant ChP_GWLs occurred in >80 % of the monitoring wells. More specifically, the ChP_GWL was observed in 2004–2005 in 81 % of the monitoring wells, in 2008–2009 in 83 % of the monitoring

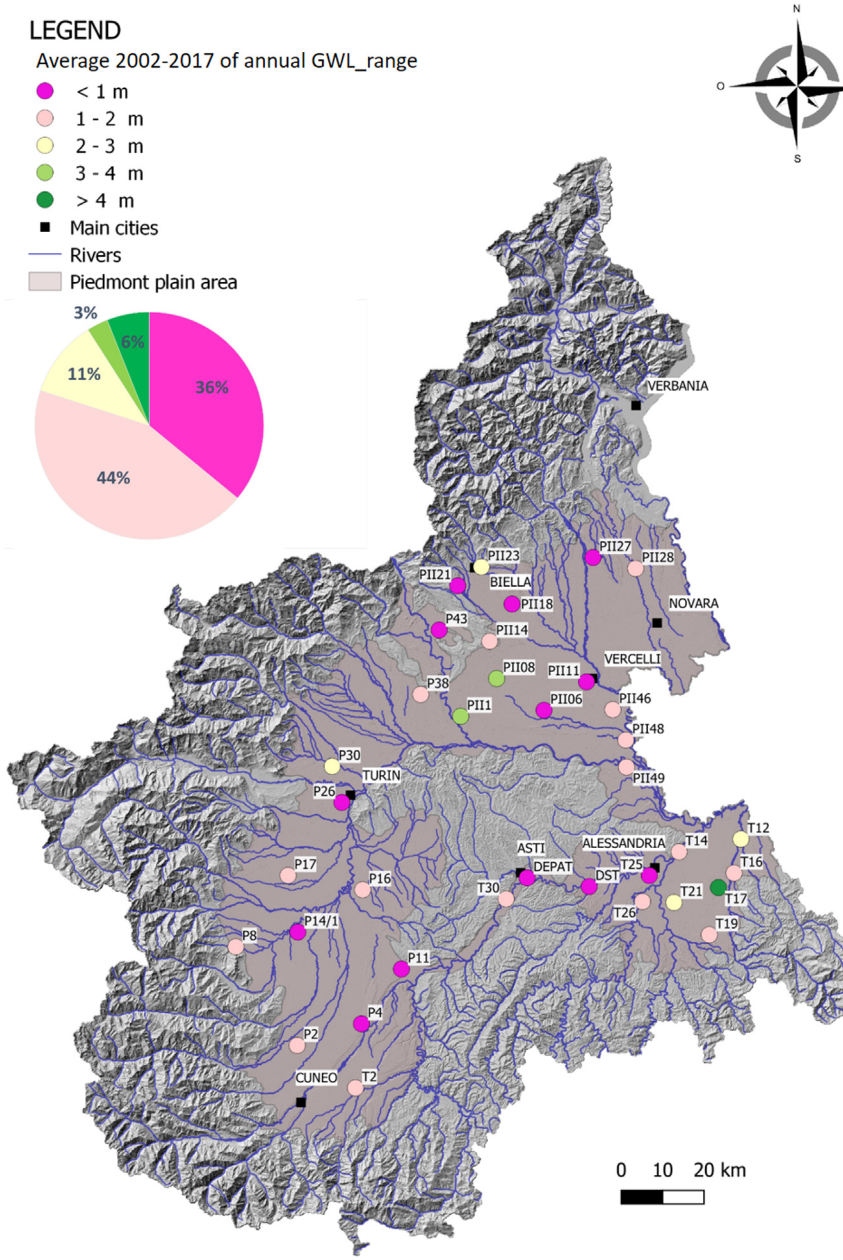

Fig. 5. Spatial distribution of average 2002–2017 of annual GWL_range fluctuations.

wells and in 2015–2016 in 86 % of the monitoring wells (Table 3a, b, c, in Supplementary material).

The most evident ChP-GWL was in 2008–2009, as also observed in the same study area by Lasagna et al. (2020b), and corresponds to the transition from a strong lowering followed by a sudden and considerable increase in the GWL (Fig. 8a). This "leap" was observed in 33 of the 36 investigated wells. More specifically, the evaluated leap was lower than 0.5 m in 13 monitoring wells, between 0.5 and 1 m in 9 monitoring wells and >1 m in 11 monitoring wells (Fig. 8b).

In the R time series, statistically significant change points (ChP_R) occurred in 19 % of the rain gauges for 2004, in 81 % of the rain gauges for 2008 and in 23 % of the rain gauges for 2015 (Table 4, in Supplementary materials). The presence of a common change point in most of the GWL and R time series suggests the close dependence of GWL on R.

The spatial distribution of ChP_GWL of 2008–2009 allowed us to identify 4 ChP_GWL (Fig. 9a): 1) ChP_GWL in April–May 2008; 2) ChP_GWL between October and December 2008; 3) ChP_GWL between January and March 2009; and 4) ChP_GWL in April–June 2009. The first group corresponds to wells located in the northeastern sector of the Piedmont Plain (in the Biella, Novara and Vercelli areas) (20 % of the total wells). The second group are wells located mostly in the southeastern sector of the Piedmont Plain (Alessandria Plain) and subordinately in the southwestern sector (Cuneo Plain) (42 % of the total wells). The third group consists of wells located in the southwestern sector of the Piedmont Plain (mostly of the Cuneo Plain) (11 % of the total wells). Last, the fourth group includes wells located principally in the northern Turin Plain (8 % of the total wells). Nineteen percent of the GWL time series showed no ChPs in 2009 and were located mostly in the Vercelli and Biella plains.

In the R time series, 57 % of the change points detected in 2008 occurred in March, and 43 % occurred in October. In particular, change points in March 2008 are referred to as rain gauges located in the central-northern sector of the Piedmont plain (Vercelli and Novara plain, Turin plain); change points in October 2008 are observed in the southern sector of the plain (Alessandria and Cuneo plain) (Fig. 9b).

In all cases, ChP_GWL showed a delay from ChP_R. Fifty percent of the delays varied from 0 to 2 months and were detected in the Alessandria

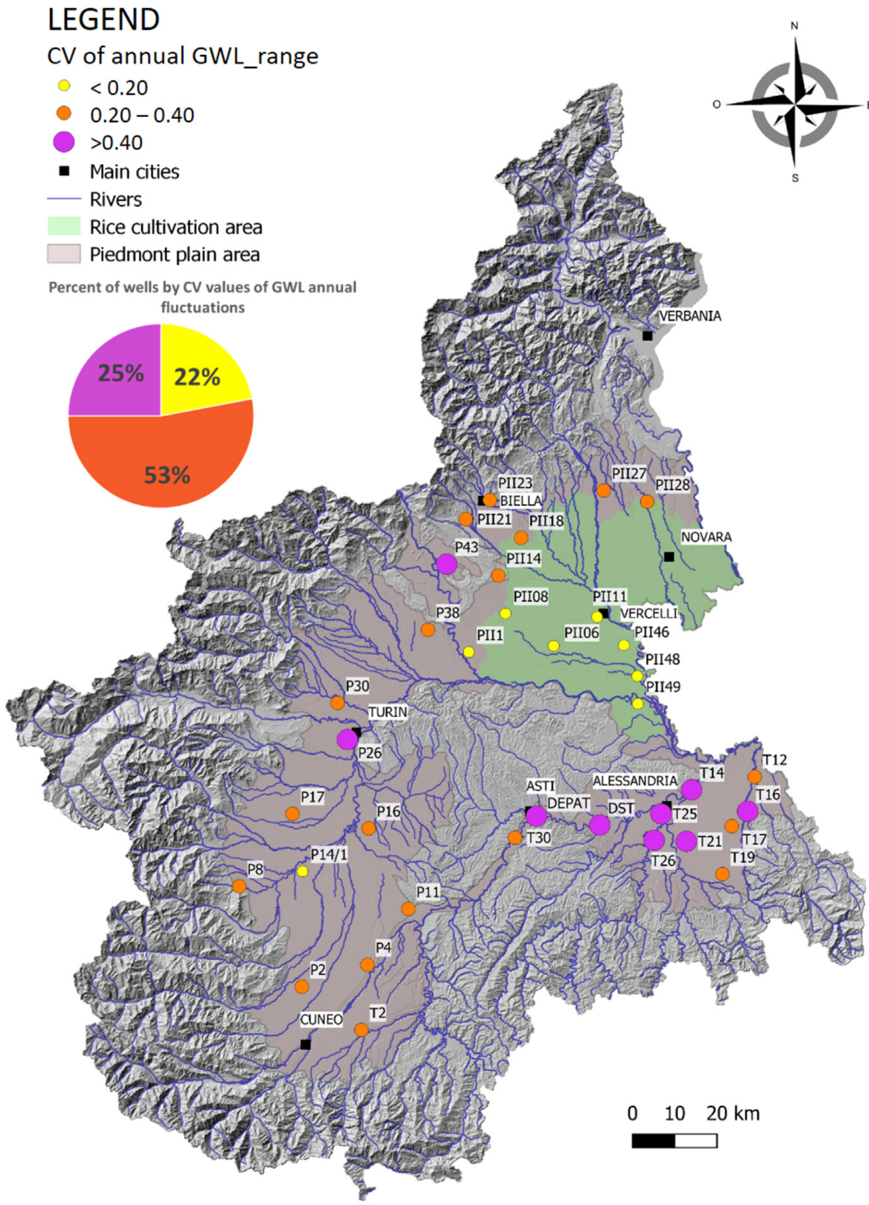

Fig. 6. Spatial distribution of the CV_GWL (CV of annual GWL_range in 2002–2017 period).

Plain and Novara and Vercelli Plains; 22 % of the delays varied from 3 to 6 months and were mostly in the Cuneo Plain and in the Biella area. Only 3 wells showed a delay higher than 1 year (from 13 to 15 months) and were located in the northern sector of the Turin Plain.

3.3. Trend analysis results

T on GWL (GWL_T) and R (R_T) were conducted for the entire observation period (2002–2017) and for the two subperiods obtained by dividing the R and GWL time series at change points ChP_R and ChP_GWL detected in 2008–2009.

GWL_T in the period 2002–2017 highlighted the presence (Fig. 10) of an upwards trend at the =0.05 level of significance in 19 % of the total wells (variation between +0.01 m/yr and +0.09 m/yr) and a downwards trend at the =0.05 level of significance in 17 % of the total wells (−0.01 m/yr to −0.14 m/yr). The other 64 % of monitoring wells did not show a trend (Table 5a, b, c, d, in Supplementary materials). Similar results were found in a previous research conducted on the same study area (Lasagna et al., 2019).

The spatial distribution of GWL_T (2002–2017) did not show a trend in the Cuneo and Novara Plains and a variable distribution of positive and negative GWL_T in the other part of the Piedmont Plain. In the Alessandria Plain, the general trend (2002–2017) of the GWL showed negative slopes in almost all cases (even if not statistically significant), with the highest decrease rate (equal to −0.14 m/yr in T17). Only one well showed a positive trend (T25 with an increasing rate of 0.01 m/yr).

In the southern part of the Turin Plain, the GWL_T (2002–2017) showed positive trends (from +0.05 to +0.09 m/yr), also in correspondence to the city of Turin. Groundwater level rise in urban areas was observed in many cities in Italy. For example, around the city of Naples (southern Italy) a progressive rising of groundwater levels started since the early 90s, reaching a maximum value of about 14 m (Allocca and Celico, 2008). The same situation was observed in correspondence to Milan (northern Italy) (Beretta et al., 2004). This phenomenon was generally attributed to a drastic reduction of groundwater withdrawal from public and private wells, formerly used for drinking water, agriculture and industry supplies.

R did not show a trend in the period 2002–2017 in all cases (Table 6 in Supplementary materials). The same results for R were obtained on the same study area by Lasagna et al. (2019).

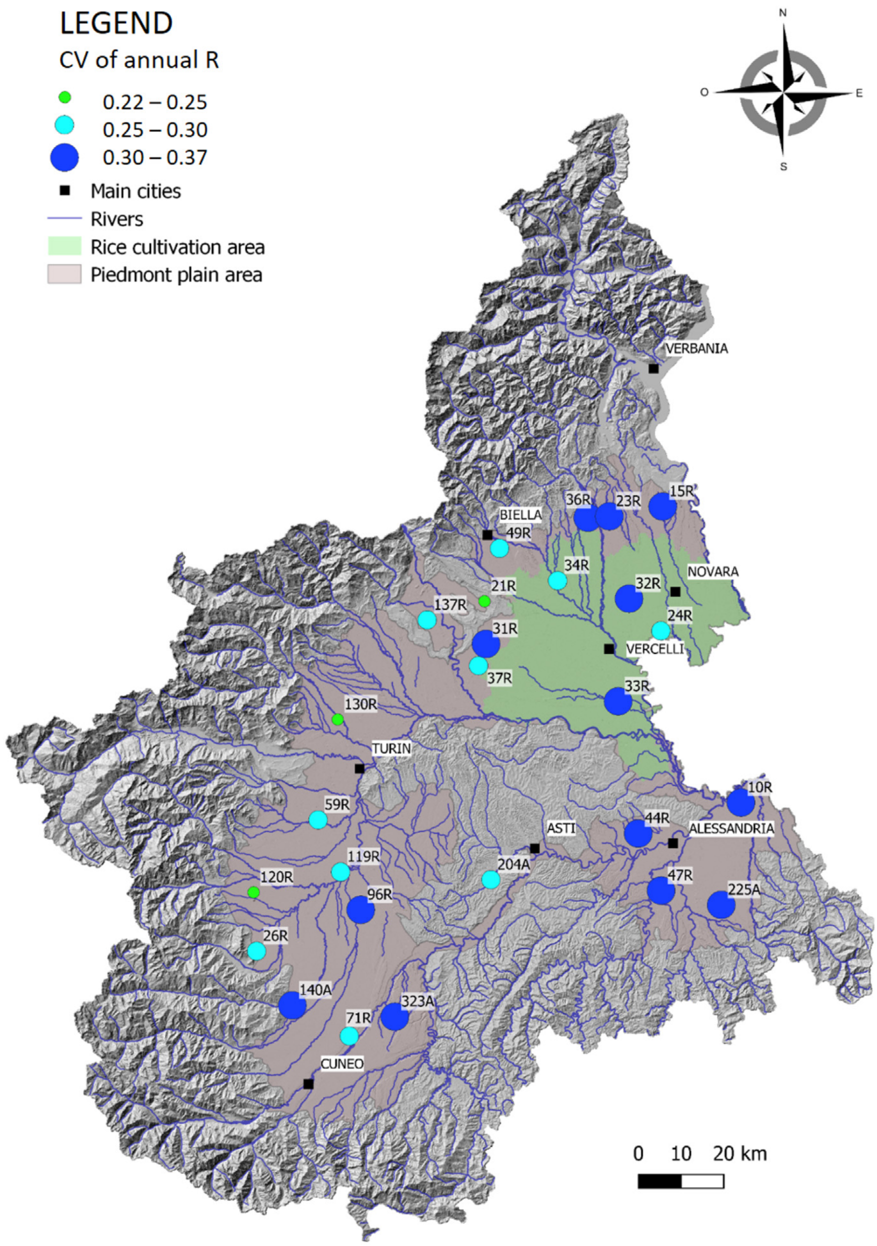

Fig. 7. Spatial distribution of CV_R (CV of annual R) in 2002–2017 period.

In the 2002–2008 period, decreasing trends in the GWL series were observed in 89 % of the monitoring wells. The other 11 % did not show a trend (Fig. 11a). No increase in GWL_T was detected. The magnitude of the negative GWL_T varied from −0.61 m/yr to −0.02 m/yr.

The spatial distribution map of GWL_T did not show a trend in the Vercelli and Novara plains. The remaining points in the Piedmont plain showed a small decreasing trend (from −0.04 to −0.12 m/yr). Decreasing GWL_T in the Cuneo Plain ranges between −0.05 and −0.20 m/yr (only well P2 showed a strong negative trend of −0.61 m/yr). The highest negative GWL_T was detected in the Alessandria Plain and along the western foot mountains (from −0.10 to −0.42 m/yr).

Decreasing trends in R in the 2002–2008 period were recorded at 38 % of the rain gauges (Fig. 11b) and did not show a trend in the other R time series. The magnitude of decreasing R_T varied between −2.4 mm/yr and −10.9 mm/yr.

In the 2009–2017 period, a decrease in GWL_T was observed in 80 % of the monitoring wells, a positive trend in 3 % of the monitoring wells and there is not a trend in the other GWL time series (Fig. 12a). The magnitude of decreasing GWL_T varied between −0.02 m/yr and −0.42 m/yr. The most pronounced lowering of the GWL is in the Alessandria Plain. In the Vercelli and Novara plains, a decreasing GW_T was present in both the analyzed intervals (2002–2008 and 2009–2017), except for the paddy fields area, where there is not a trend in the GWL time series. The same result was obtained by De Luca et al. (2005) for the period 1968–2004.

In the 2009–2017 period, decreasing trends in R were recorded at 31 % of the rain gauges, and the other 69 % did not show a trend (Fig. 12b). The magnitude of decreasing R_T varied between −2.2 mm/yr and −5.6 mm/yr. The negative R_T values were located in the eastern part of the Piedmont Plain.

3.4. Percentiles method results

The PCTL method for 2017 highlighted a general situation of GW depletion compared to the natural fluctuation of GWL. More specifically,

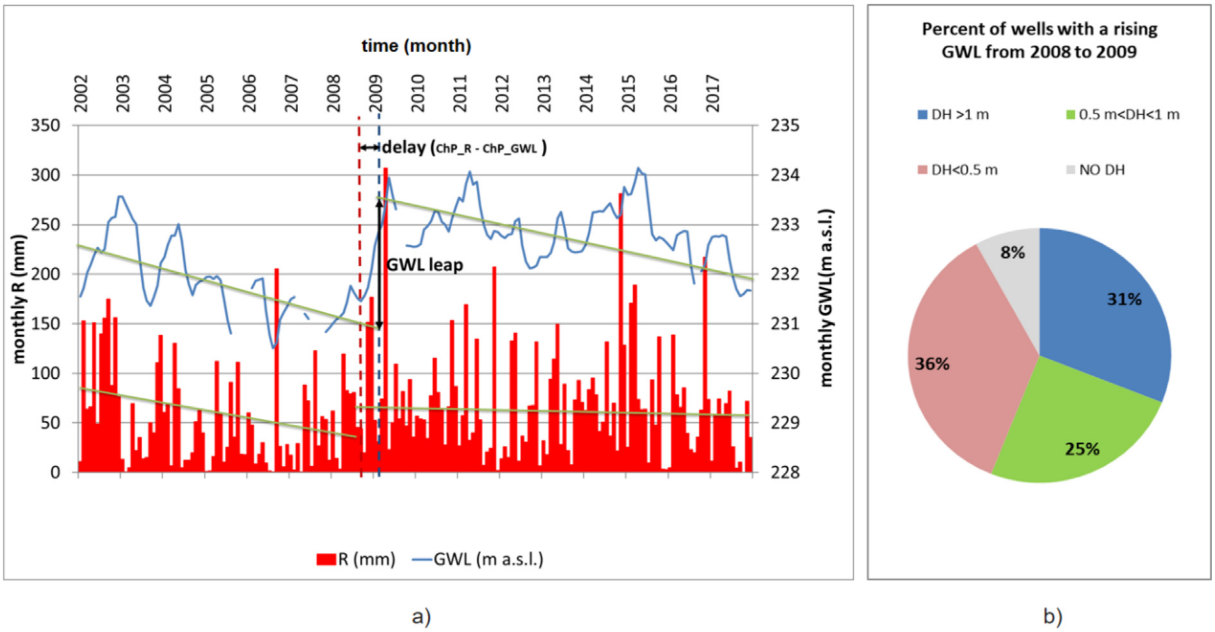

Fig. 8. a) Change_point GWL time-series (blue line) and R time series (red bar). The dashed vertical lines correspond to the dates respectively of ChP_R (red) and ChP_GWL (blue). The delay between R and GWL correspond to the difference between ChP_R and ChP_GWL (horizontal black arrow). The vertical black arrow corresponds to the leap of the ChP_GWL from 2008 to 2009. b) Percent of wells with a rising GWL from 2008 to 2009, and indication of the magnitude of GWL increase (DH) in meter.

only 8 % of the monitoring wells had all monthly GWLs in the range of the natural fluctuation (Fig. 13). These monitoring wells are located in the western part of the Piedmont plain (south of Turin). Ninety-two percent of wells showed at least 1 month below the reference threshold (15 % of the range of the natural fluctuation) and were then considered critical: 25 % of wells showed from 1 to 4 months, 42 % of wells showed 5–8 months

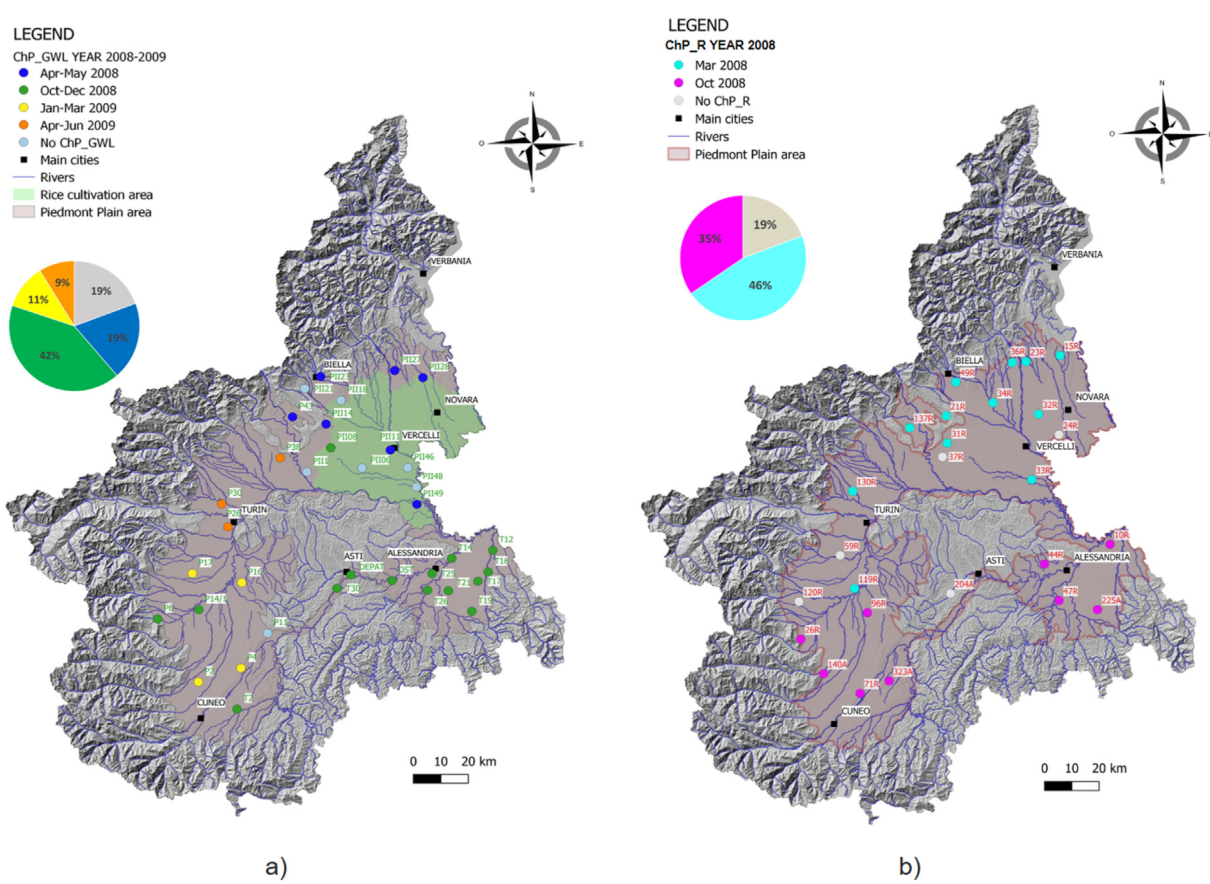

Fig. 9. Spatial distribution of 2008 a) ChP_GWL and b) ChP_R in the Piedmont Plain and percent of wells/rain gauges subdivided according to the date on which the ChP occurred.

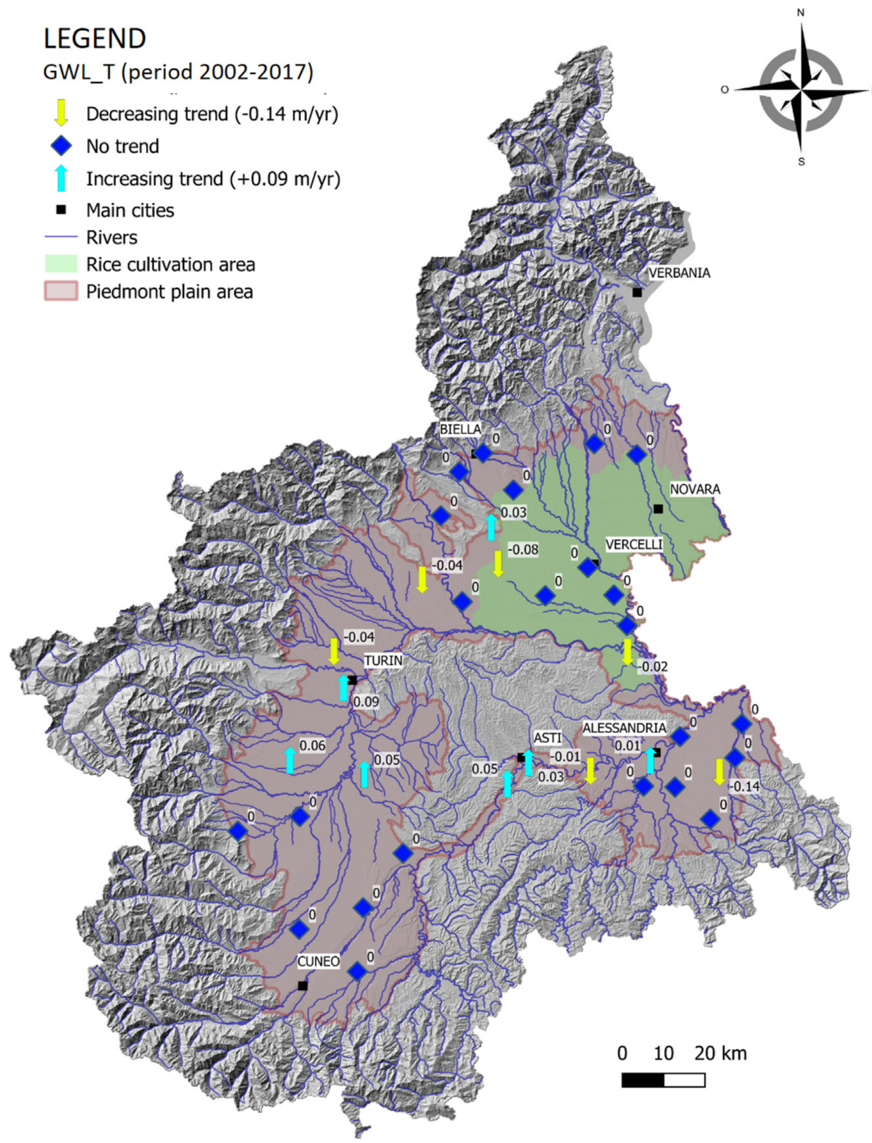

Fig. 10. Spatial distribution of the GWL_T in the 2002–2017 period in the Piedmont Plain. In the 2002–2017 R did not show a trend.

and 25 % of wells showed from 9 to 12 months below the reference threshold. The most critical conditions were found in the southeastern sector of the Piedmont plain (Alessandria Plain). Almost all wells in Alessandria (with the exception of well T14) and Asti plains showed a minimum of 7 months to the full year 2017 below the identified threshold. In this area, the months below the threshold always correspond to the summer and autumn seasons (from May to December).

In general, in 2017, wells in the Piedmont plain most frequently showed 4 to 6 months below the reference threshold in correspondence with the second part of the year, with more accentuated lowering in the months from April to December (Fig. 14a, b, d). Some wells located in the Vercelli paddy field area are an exception, showing above-threshold values in the summer months (May to September), probably linked to the period of flooding of the paddy fields (Fig. 14c).

The wells located in the lowland sector south of Turin mostly showed all months with GWL values above the threshold values (Fig. 14d).

3.5. Non-standardized anomalies

The non-standardized anomalies (or anomalies) allow us to quantify the deviation, positive or negative, of the GWL from the reference level for each monitoring point.

Annual GWL anomalies (GWL_AN) allow us to identify years characterized by GW deficits or exceeds and to quantify yearly deviations (Fig. 15a, c, e, g). The annual R anomalies (R_AN) allow the detection of dry and wet years and the quantification of the yearly deviations (Fig. 15b, d, f, h).

The analysis of annual GWL_AN for 2017 showed values below the reference levels that varied between −0.06 and −2.80 m in 92 % of wells (Table 7 in supplementary materials). The most critical conditions were located in the southeastern sector of the Piedmont Plain (Alessandria) (Fig. 16a). Only 8 % of wells showed an annual GWL_AN above the reference level, with values that ranged between +0.20 m and +0.40 m.

The R for 2017 showed, in all cases, negative annual R_AN with values below the rainfall reference levels that vary between −147 and −536 mm (Fig. 16b and Table 8 in Supplementary materials). The greatest pluviometric deficits in 2017 were located in the northeastern sector of the Piedmont Plain (Novara and Vercelli).

In 2017, the spatial distribution of GWL_AN generally showed different values in the different sectors of the Piedmont Plain.

In the Novara and Vercelli paddy field areas, the yearly GWL_AN was close to the reference level (Fig. 15a), and in 2017, all the monitoring wells, except for PII08, had anomalies <0.6 m (Fig. 16a).

In the Cuneo Plain, the yearly GWL_AN was nearly the reference level but, in general, was more pronounced than in the Vercelli Plain (Fig. 15c), and in

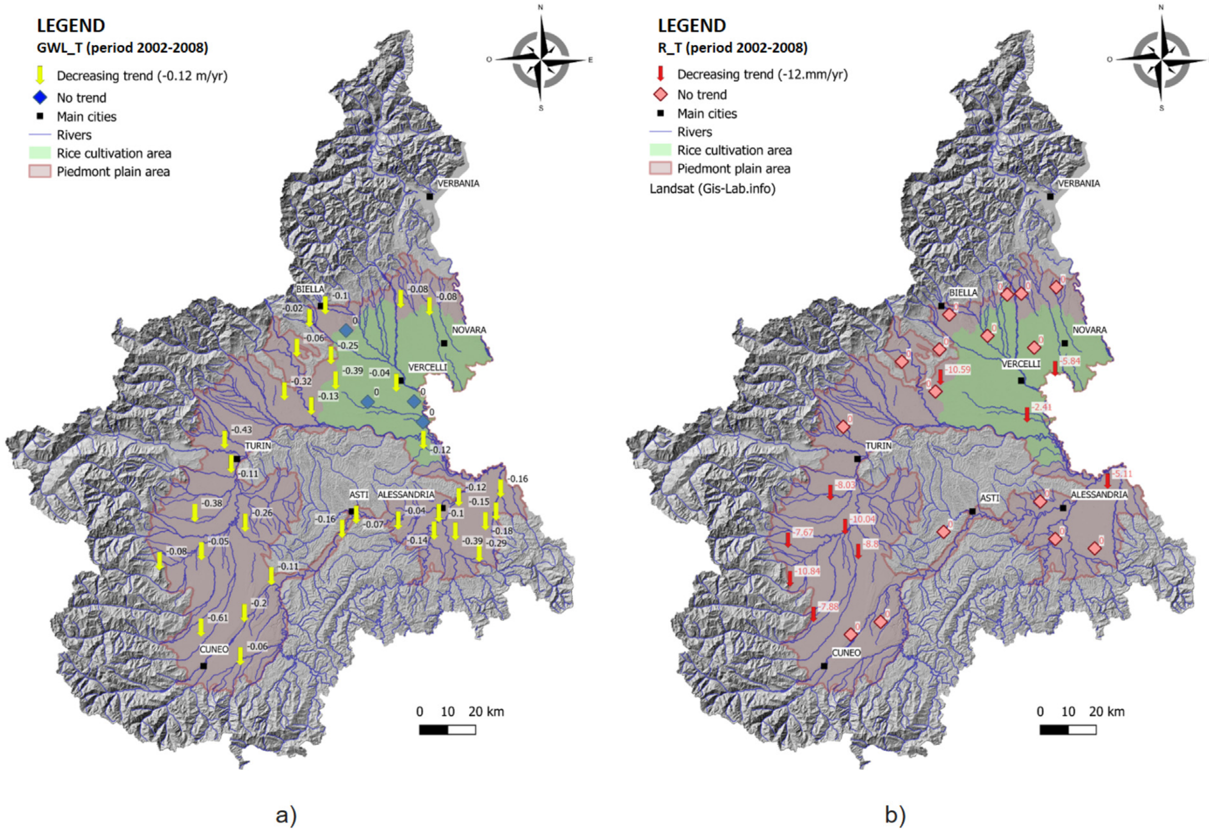

Fig. 11. Spatial distribution of a) GWL_T and b) R_T in Piedmont Plain in the period 2002–2008.

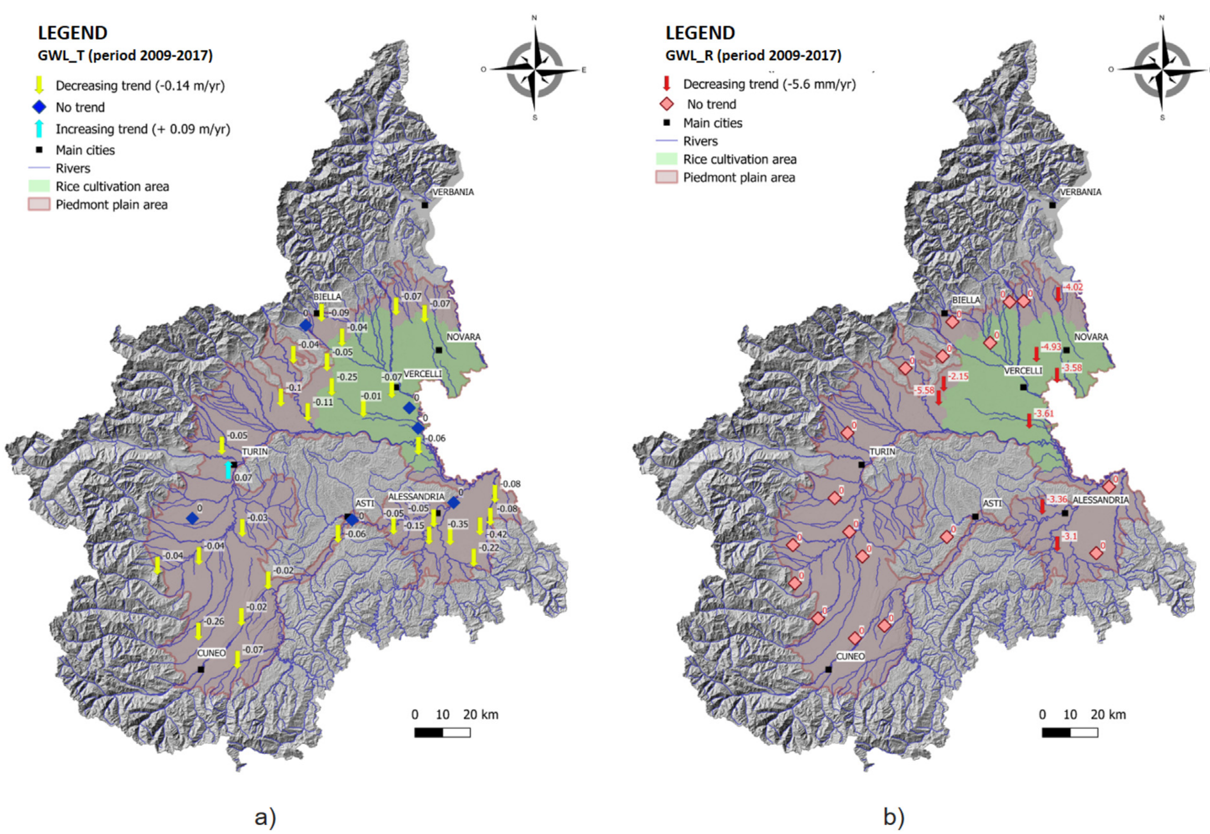

Fig. 12. Spatial distribution of a) GWL_T and b) R_T in Piedmont Plain in the period 2009–2017.

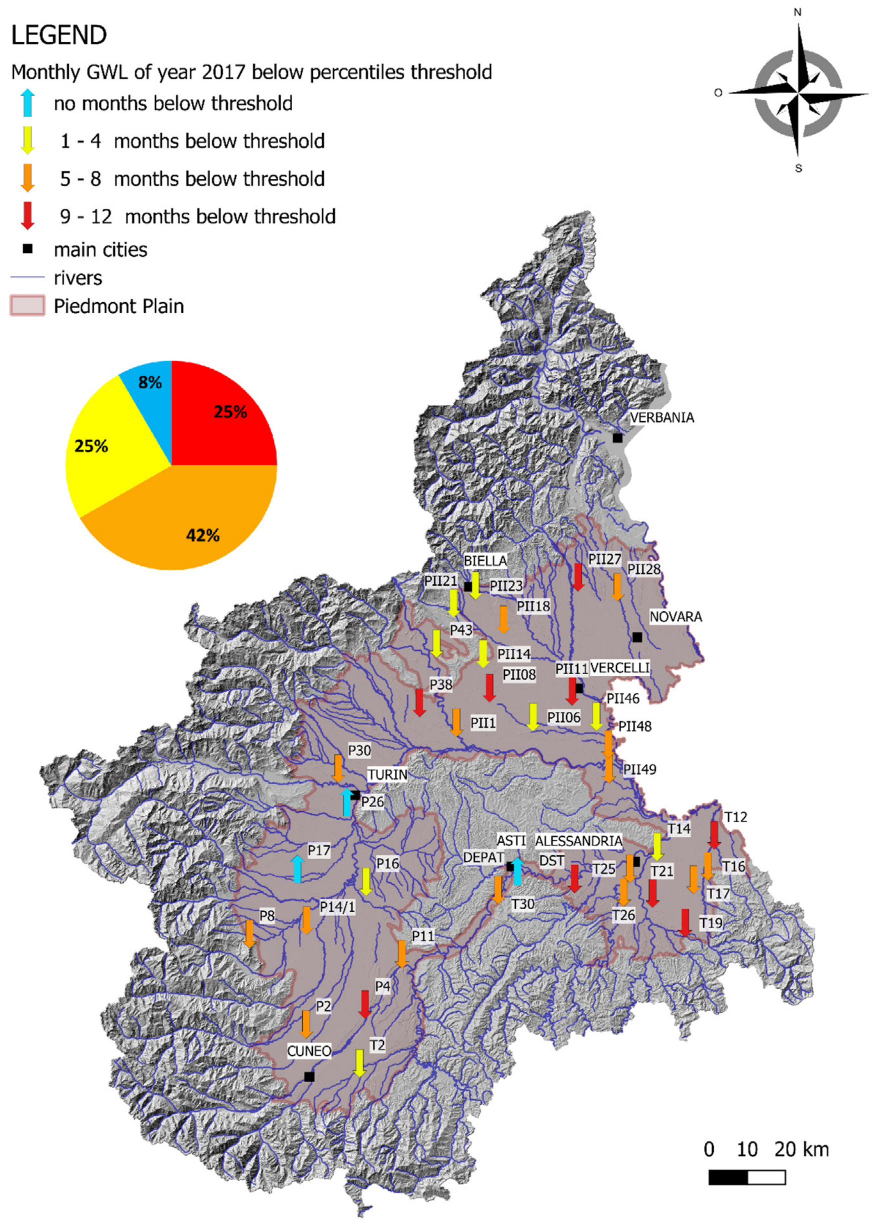

Fig. 13. Spatial distribution of wells with 2017 monthly GWL below the percentile thresholds (15 % of natural fluctuation) and number of months (arrow down). Percent of wells with number of months with GWL below the percentile threshold.

2017, all the monitoring wells showed a negative GWL_AN of <0.8 m (Fig. 16a).

On the Alessandria Plain, the yearly GWL_AN showed the highest negative values, and in 2017, several monitoring wells showed negative GWL_AN values of >1.4 m up to 2.8 m (Fig. 16e). The wells located in the Tanaro valley showed a 2017 GWL_AN of a few tens of centimeters (0.10–0.30 m) (Fig. 16a).

Positive and negative GWL_AN were detected in some wells in the southern part of the Turin Plain (Fig. 15g and Fig. 16a) with annual values lower than 0.4 m in 2017.

The comparison of annual R_AN with GWL_AN shows that large R_AN values do not always correspond to large GWL_AN values. Generally, R_AN had the same sign as GWL_AN (Fig. 15b, d, f, h). Sometimes, it was possible to observe a lag of 1 year.

A positive R_AN corresponded to the wet period and was observed in 2002, 2008–2011 and 2013–2014. Negative R_AN, corresponding to the dry period, was observed in 2003–2008 and in 2017. The years 2015 and 2016 showed a positive R_AN in the Turin and Cuneo Plains (western Piedmont Plain) and a negative R_AN in the Vercelli and Alessandria Plains (eastern Piedmont Plain).

4. Discussion

The application of different methods (such as T, ChPA, PCTL, AN and the analysis of annual fluctuations and their variations over time) to the GWL series of the Piedmont Plain allowed us to assess the GWL evolution over time.

Variations in GWL depend on many factors related to the hydrogeological context, climate and anthropogenic pressures and their variability over time. Moreover, the application of these methods to the R time series also allowed the comparison between R and GWL results, providing further information on the hydrodynamic behaviour of groundwater and on its link with R variability.

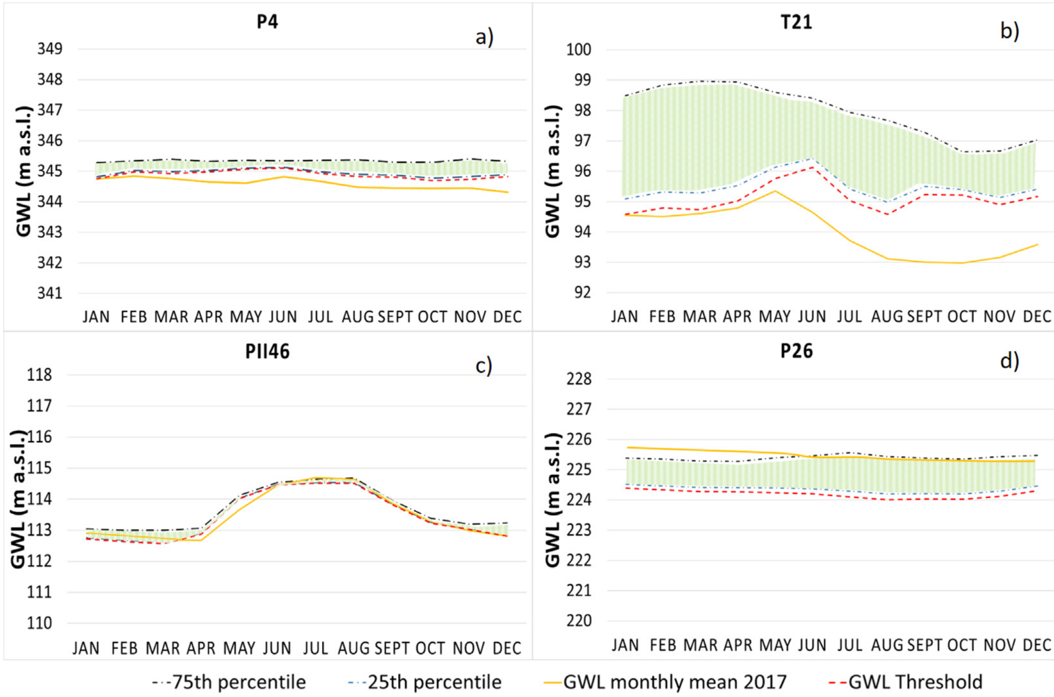

Fig. 14. a) Examples of monitoring wells with the indication of the 25th and 75th percentiles (respectively the blue and black dotted lines), the GWL natural fluctuation band (green area), the "ISPRA" threshold computed as 15 % of natural fluctuation (red dashed line), and monthly GWL of 2017 (yellow line): a) Cuneo Plain (P4) with 12 months below the threshold; b) Alessandria Plain (T21) with 12 months below the threshold; c) Vercelli Plain (PII46) with 3 months below the threshold; d) Turin Plain (P26) with 12 months above the threshold.

Furthermore, the spatialization of the GWL elaborations allowed us to identify the most critical areas and the potential factors (anthropic, geological and hydrogeological) conditioning the hydrodynamic GWL behaviors.

Finally, this multicriteria approach, considering the same time interval, allowed us to highlight the advantages and limits of the applied methods.

4.1. The evolution of the GWL

The T conducted in the period 2002–2017 indicate that all rain gauges and approximately half of the monitoring wells did not show any trend. Nineteen percent of the total wells showed a positive trend, and only 17 % of the total wells showed a negative trend. Since the results of T depend on the time interval considered, especially in cases where the slopes are not accentuated and in the case in which the interval is not so long, it was useful to search for change points to define the beginning or the end of the analysis intervals.

The presence of the change point in 2008 allowed us to divide the time series into two parts, and T was applied to the two subperiods showing a general decreasing trend in >80 % of wells and in <35 % of rain gauges. Generally, the negative GWL_T detected in 2009–2017 showed fewer negative slopes than those detected in 2002–2008. Moreover, aquifer responses also seem to be different in similar climatic areas.

The trends obtained for the second subperiod (2009–2017) were comparable with the results obtained by applying the percentile method and the non-standardized anomaly method.

The PCTL highlighted a general situation of GW depletion in only 11 % of wells showing a piezometric level above the threshold and in the range of the GWL natural fluctuation. The analysis of GWL_AN for 2017 confirmed the results of percentiles, showing annual values below the reference level that vary between 0.2 and 2.8 m in 92 % of wells (Table 7 in Supplementary materials). Moreover, percentile analysis for 2017 showed that the greatest GW deficits generally occurred in the second part of the year.

The R for 2017 showed, at all rain gauges, negative anomalies that varied between −147.26 mm in the Alessandria Plain and −585.21 mm in the northern area of the Piedmont Plain (Novara and Vercelli areas). This deficit in the R can be the cause of the GW depletion in 2017.

4.2. Comparisons and relationships between R and GWL fluctuations

The analysis of the maximum amplitude of annual GWL fluctuation (GWL_range) showed that this value varies over time and that most of the analyzed wells had an average GWL_range lower than 2 m (80 % of the wells). During the analyzed period, the maxima of GWL_range were generally observed in the years 2002–2003 for 47 % of the monitoring wells and secondarily in 2009 (8 %) and 2013–2014 (14 %); minimum values of GWL_range were, instead, more distributed over the years. However, a high presence of the minimum GWL_range in 2007 and 2013 can be observed (Table 1 in supplementary materials). To explain the periods of maxima and minima annual amplitude of GWL fluctuations, a comparison with average annual R was performed.

The high fluctuations in the highlighted periods can be ascribed to particularly high R (up to 1400 mm/yr) or low R (<800 mm/yr) with respect to the average annual R in the Piedmont Plain (911 mm/yr, Fig. 2). Periods of high R are effectively identified in 2002, 2008–2010 and 2014, whereas low R are measured in 2003–2007 and 2017. In contrast, the minimum amplitude of annual GWL fluctuations seems not linked to periods of particularly elevated or low R.

The CV_GWL allowed us to evaluate the interannual variation degree of the GWL_range in each monitoring well. Then, the spatialization of the CV_GWL allowed us to identify areas with the highest interannual variation (CV_GWL > 0.40 in the Alessandria Plain), areas with the lowest interannual variation (CV_GWL < 0.20 in the Vercelli and Novara plains) and areas with intermediate CV_GWL values (0.20 < CV_GWL < 0.40). The interannual variation in R showed medium-high CV_R values (from 0.22 to 0.37), with the highest variations in the Alessandria, Cuneo, Novara and Vercelli plains.

By comparing CV_GWL and CV_R, it was possible to distinguish areas with comparable interannual variability. The highest values of CV_GWL

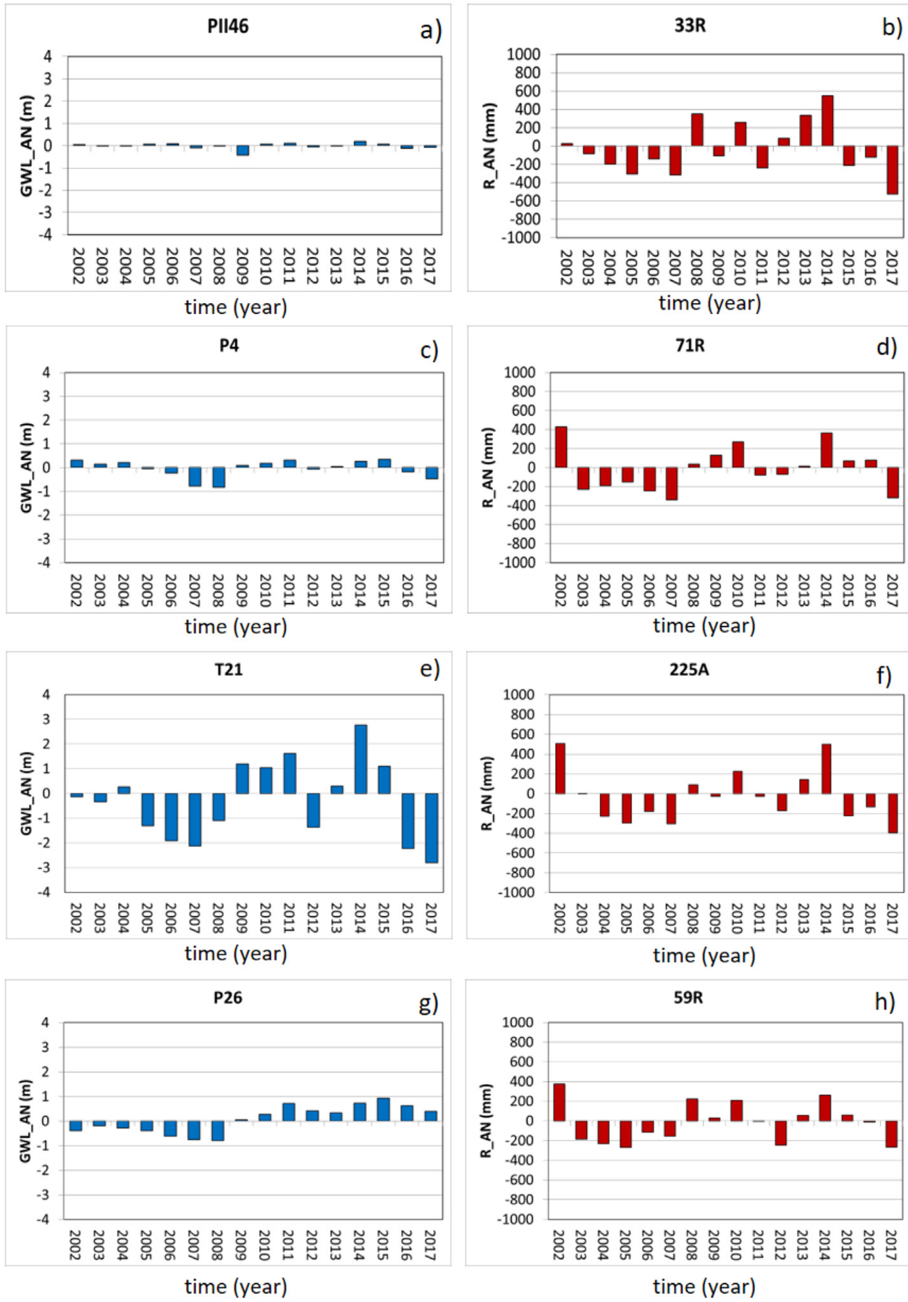

Fig. 15. Annual GWL_AN (blue bar) and annual R_AN (red bar) of monitoring wells and correspondent rain gauges, respectively: a) and b) in the Novara-Vercelli Plain; c) and d in the Cuneo Plain; e) and f) in the Alessandria Plain; g) and h) in the Turin Plain.

and CV_R were detected in the Alessandria Plain, suggesting a rather close link between R and GWL variation; however, the variation in the annual cumulative R was lower than the variation in the annual excursion of the water table (CV_GWL > 0.40 and CV_R > 0.30).

In contrast, in the Novara and Vercelli plains, it was observed that the annual GWL_ranges varied little over time (CV_GWL < 0.20) and, in any case, were less than the variability in R (CV_R > 0.30). The low CV_GWL could be explained by systematic paddy field flooding (Lasagna et al., 2020b), which influences and controls the variations in the water table in the spring-summer period. The water used for the permanent flooding of the rice fields is derived from rivers in the northern part of the area and through a network of channels managed by local irrigation authorities.

The analyses of change points in GWL and R highlighted a common change point in 2008–2009 for most analyzed series. This testifies that the water table oscillation is ruled more or less evidence by R, which is expected. Most specifically, the highlighted rise in the GWL in 2008–2009 can be explained by a considerable increase in precipitation. Observing the annual R in the Piedmont plain, it is possible to point out that 2007 was a particularly dry year (with average R values below 650 mm), while 2008 was a rainy year (with average R values above 1100 mm). In addition, according to what was reported by ARPA (ARPA, 2016), 2008 was, on a regional scale, the second year with the largest anomaly of positive snowfall since 1950. Consequently, it cannot be excluded that the melting of these snows contributed to the rapid rise recorded in 2009. However, this does not mean that the variations in the GWL are due exclusively to precipitation. In all cases, Chp_GWL shows a delay time compared to the dates of ChP_R. Minor delays (0–3 months in the Alessandria and Novara and Vercelli Plains) could indicate a speed recharge of the aquifer by R, favored by depths of GWL and high permeability of the unsaturated soil. Higher delays (over 3–6 months) could indicate a

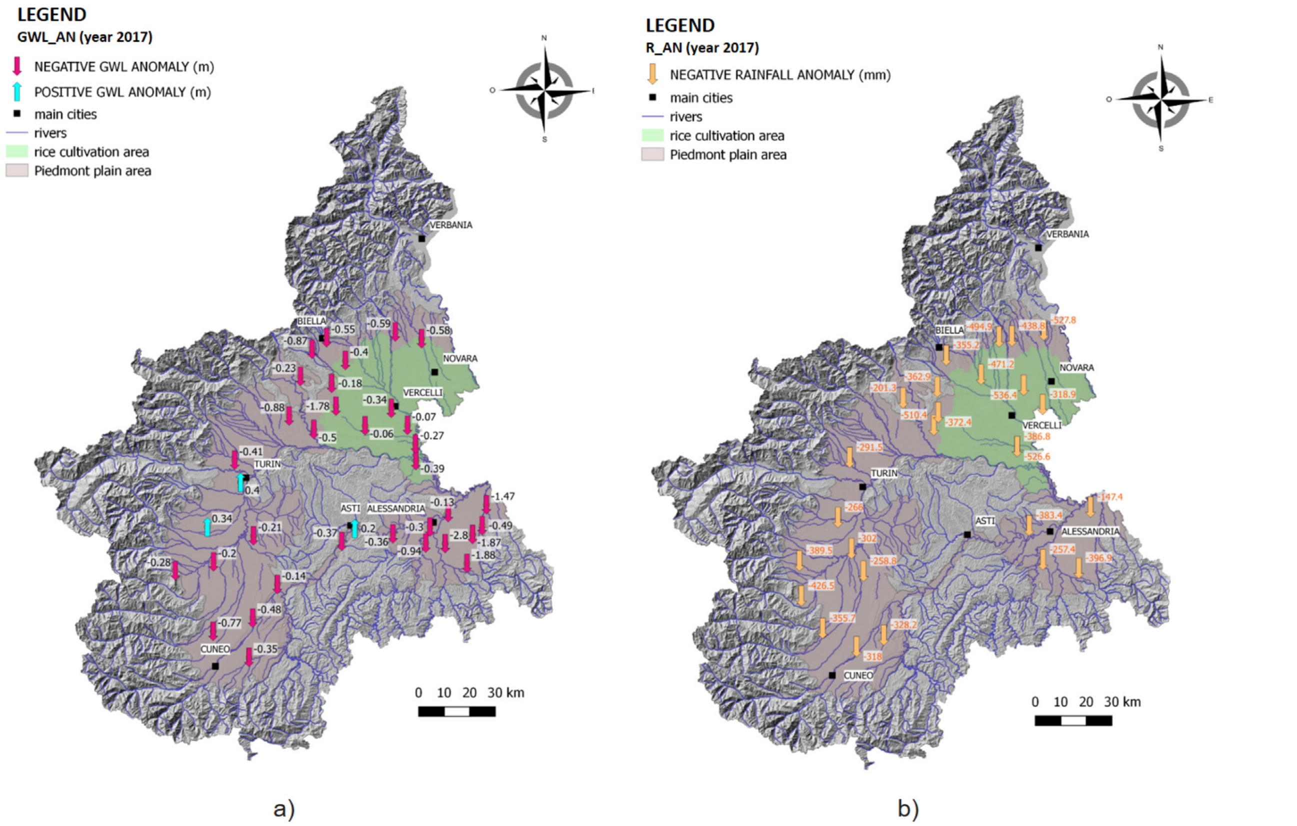

Fig. 16. Spatial distribution for the year 2017 of a) GWL_AN. Negative GWL_AN (red arrow down) and positive GWL_AN (blue arrow up); b) R_AN. R showed, in all cases, a negative anomaly (yellow arrow).

higher influence of further factors in addition to rain, such as permeability of the unsaturated soil, depth of the water table, snow melt, irrigation, and anthropic water depletion. For example, well P38 has the greatest depth of the water table (47 m) and has a delay of >12 months.

4.3. Quantitative status of GW resources in the Piedmont Plain

The analysis of the GWL over time permitted us to define the quantitative status of the GW resources for 2017, identifying 4 different plain areas with similar behaviors (Fig. 17):

a) Southeastern sector (Alessandria plain),
b) Northeastern sector (Vercelli-Novara plain with rice fields),
c) Northwestern sector (Turin plain),
d) Southwestern sector (Cuneo Plain).

It should be noted that 2017 in the Piedmont Region was the 3rd warmest year in the last 60 years, with a thermal anomaly of approximately $+1.5$ °C compared to the climatology of the period 1971–2000 and the 4th driest year of the last 60 years (ARPA, 2018). However, aquifer responses also seem to be different in similar climatic areas.

4.3.1.1. Southeastern sector (the Alessandria plain). The Alessandria plain is located on the border with the Apennine chain and is characterized by a local climate that is different from the other parts of the Piedmont Plain. More specifically, it is characterized by the lowest average annual R (of the Piedmont Plain) and the highest summer temperatures (which probably also intensify water withdrawals in the area as well as affect evapotranspiration). The particular location and geometry of the aquifer are characterized by a small areal size, as it is surrounded to the northwest and south by the BTP sedimentary rocks.

In 2017, all the methods applied to the GWL identified a critical situation in this plain. R variations and other factors, such as the increase in withdrawals from the aquifer principally due to the drought that characterized this area (Regione Piemonte, 2020), are likely to contribute to the pronounced decline in GWL.

All GWL_T analyses showed the maximum negative slope (max $= -0.42$ m/yr for GWL_T$_{2008–2017}$) in the Alessandria Plain, and percentile analysis and GWL_AN (max $= -2.80$ m) identified the most critical conditions in this area (for 2017). The analysis of the interannual variation in GWL_range and annual R amounts showed the highest values in the Alessandria Plain (CV_GWL > 0.40 and CV_R > 0.30), suggesting a rather close link between R and GWL variation.

The GWL depths in this area are between 5 and 11 m below the ground surface, and these data can in part justify the low time response (0–2 months) of the GWL to R.

4.3.1.2. Northeastern sector (Vercelli-Novara plain). The northeastern sector of the Piedmont Plain is characterized by an average depth of the water table lower than 5 m below the ground surface and a generally high hydraulic conductivity of soils (De Luca et al., 2020). The aquifer is bounded to the north by the mountain chains of the Alps and to the south by the Monferrato hills, at the base of which flows the River Po. The Vercelli and Novara areas were largely characterized by the presence of paddy fields that were subject to repeated flooding phases during the period from April to August. During flooding, the water table is artificially fed, thus reducing/masking any criticalities arising from a scarce natural recharge.

The Novara and Vercelli plains showed the highest annual R compared to other areas of the Piedmont Plain. The GWL_T analysis in this area did not show a trend for the period (GWL_T$_{2002–2017}$) but a negative trend in the second subperiod (GWL_T$_{2008–2017}$), with most slopes below 0.1 m/yr. The time response of GWL to R varies from 1 to 2 months and seems to indicate that the effects of R become evident quickly. Despite the shallow water table and the high hydraulic conductivity of the soils, the time response is greater than those evaluated in the Alessandria area, where the

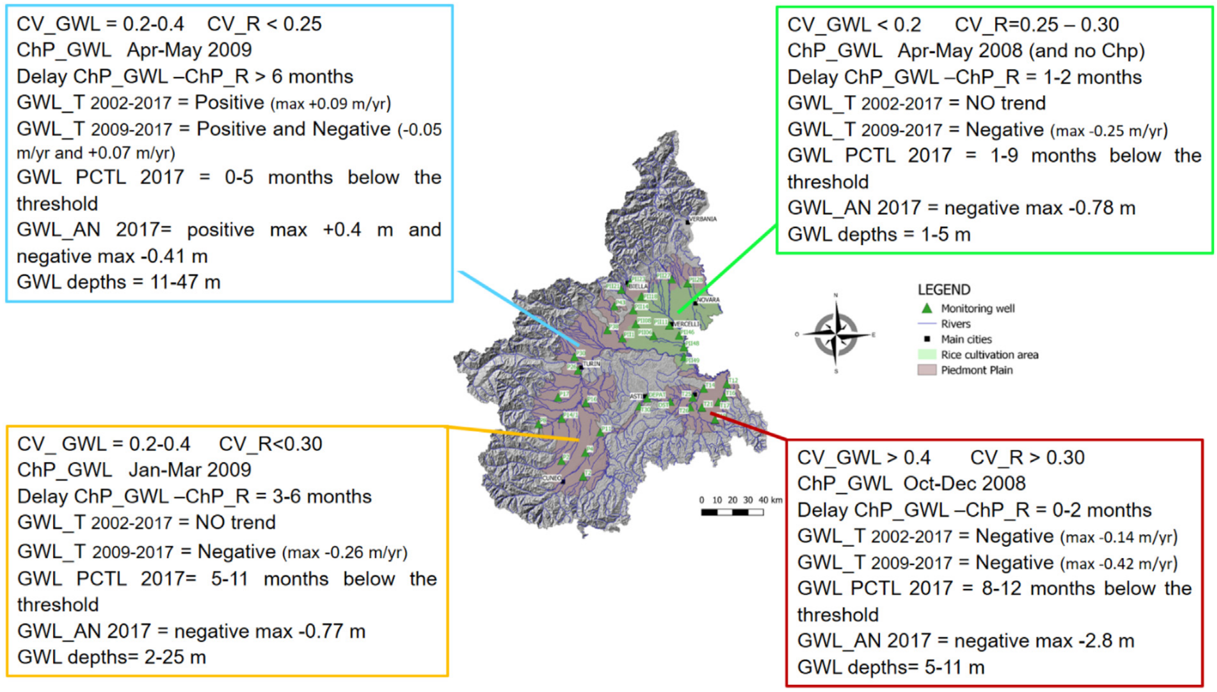

Fig. 17. Summary of the main results of the different statistical elaborations and identification of 4 sectors, of the Piedmont Plain, identified by similar CV, trends, delays and, GWL_AN.

water table is mostly deeper and the hydraulic conductivity is similar. Furthermore, the interannual variability in GWL_ranges in this area is the lowest in the Piedmont Plain (CV_GWL < 0.2).

These effects could be explained by the artificial water supply that influenced and conditioned the course of the GWL during the summer period and helped to reduce the annual amplitude of GWL fluctuations, which, under natural conditions, would probably have been much higher (Lasagna et al., 2020b).

4.3.1.3. North-Western sector (Turin Plain). The Turin Plain, between the Alpine edge to the west and Turin Hill to the east, is the connecting element between the Cuneo Plain and the rest of the Po Valley. It is bordered to the west by the morainic apparatus of Rivoli-Avigliana and to the east by the hills of Turin. The subsoil has a prevalent permeability for medium grade porosity, with a frequent lower degree of hydraulic conductivity, especially in the oldest and altered terms ($10^{-7} < k < 10^{-3}$ m/s) (De Luca et al., 2020). The average depth of the water table is higher than 10 m, up to 40 m below the ground surface. The analyses conducted on the wells present in this area showed different results compared to those found in the other areas. In the southern sector, increasing trends have been identified both for the long period (2002–2017) and for the last subperiod (2009–2017); moreover, the GWL of 2017 was higher than the reference threshold calculated with the method of percentiles, and the annual GWL_AN anomalies also showed positive values (up to 0.4 m), despite the rain presenting negative annual R_ANs. The average GWL_range was generally <2 m, and CV_GWL had intermediate values (0.2 < CV < 0.4). This area is where the highest delays in the response of the GWL to R occur (over 6 months). These data could be related to deep GWL, with soils characterized by medium-low hydraulic conductivity. However, other factors could also likely explain this different behaviour.

The particular position of the lowland area with respect to the Alpine arc suggests that, perhaps, a nonnegligible water contribution could be derived from snow melt. This further contribution could partly explain the positive trends observed in the area and the moderate CV_GWL.

4.3.1.4. South-Western sector (Cuneo Plain). In the Cuneo Plain, the average depth of the water table is highly variable (from a few meters up to 24 m). In wells with a shallower water table, the amplitude of the GWL_range oscillation seems to be lower (<1 m) than in wells with a deeper water table. The interannual variation in the maximum amplitude of GWL fluctuations is intermediate (0.2 < CV_GWL <0.4) and comparable to CV_R (CV_R = 0.3). However, the delays between ChP_R and ChP_GWL varied from 3 to 6 months. This delay in the GWL response to R may be related to the depth of the water table.

The GWL_T analysis in this area did not show a trend for the long-term period observed (2002–2017) but a negative trend in the last subperiod (2009–2017) with slopes of −0.26 m/yr. The PCTL analysis applied for 2017 showed at least 5 months below the reference threshold in all wells, and negative GWL_AN was detected (max −0.77 m). The slightly negative trends recorded in the last period and the more negative anomalies calculated for 2017 can also be explained in this case, as for the Turin Plain, by a water contribution that could derive from snow melt.

4.4. Advantages and disadvantages of applied methods for GWL analyses

It is important to emphasize that all the analyzed methods, to have good and significant applicability, require a rather high number of years of measurement (on average of at least 5 years, to many decades (ISPRA, 2017)). Additionally, continuity over time of measurements is necessary, and the lack of continuity of the data as well as the high presence of missing data can distort the results. Furthermore, to make comparisons between the results of the elaborations, it is important to consider the same time interval.

The analysis of change points is useful for determining the moments when a change in trends is observed and allows the subdivision of the time series into smaller intervals. In addition, the change points search can be useful to identify and compare moments common to different time series (i.e., between R and GWL) and to evaluate the possible delay in responses. Last, the change points are sensitive to the length and time period analyzed.

The evaluation of the trends is simple and can be usefully interpreted in association with GW status data. T gives an idea of the evolution of the GWL over time. However, the evaluation of a statistically significant T, above all when the T line does not present a high slope and in the presence of not a very long temporal series, is strongly dependent on the analyzed period

(Mariani, 2006); thus, the choice of the reference period appears to be a key element for the analysis of trends. Moreover, it is advisable to evaluate the presence of change points in the GWL series and to evaluate the trends in different time intervals. Common change points detected in different time series can be considered starting (or finishing) points for T. T for the assessment of climate change impacts on groundwater recharge, groundwater level and resources, requires a long time interval (e.g. >30 years), but the observation data, e.g., groundwater levels are generally not available. Moreover, short-term T series can be used to assess the effects of climate variability and provide useful information on aquifer recharge patterns.

The percentile method proposed by ISPRA establishes an alert threshold below which the GWL is considered critical. Furthermore, the percentile method shows intuitive diagrams. However, it does not convey the extent of GW depletion. The warning threshold is determined on the basis of the amplitude of the "natural fluctuation". In the cases where the amplitude of the 'natural fluctuation' band is low, the threshold will be close to the 25th percentile, and a GWL below the defined threshold does not always correspond to a real criticality.

The assessment of the magnitude of the annual GWL_range fluctuation, of the interannual variation by means of the CV and the calculation of non-standardized anomalies can improve this method.

The application of non-standardized anomaly analysis allows us to quantify the critical issues and therefore to determine the "real" potential critical cases. The GWL_AN furnishes the deviation (positive or negative) measured in meters of the GWL from the reference GWL and allows us to examine the nature of the trends, enabling the determination of the dry and wet years. It is important to have a large reference period and to maintain this period for calculating future anomalies. Because the assessment of anomalies also depends on the reference period, it is advisable to use the same reference period for the analysis of the other climatic variables that contribute to the changes in the GWL. The evaluation of GWL_AN is easy to apply and makes the extent of the lowering more evident. The GWL_AN analysis allows us to quantify the critical issues and therefore to determine the "real" potential critical cases.

5. Conclusions

Numerous factors (hydrogeological, meteorological, anthropogenic activities) play a role in GW behaviour and have to be identified from time to time. Monitoring networks and collection of data are an important starting point for analyzing GW behaviour to better manage water resources. The application of different statistical methods to the GWL series allows us to describe the evolution of the GWL, and the spatialization of the results permits to identify areas with a similar hydrodynamic behaviour and resource evolution.

The main aims of the study were the comparison of different statistical methods, highlighting their applicability and differences, and the investigation of the spatiotemporal variation in the GWL of shallow aquifers in the Piedmont Plain, with the description of critical situations of GW depletion.

This study highlights that the application of a single method for assessing shallow GW resource evolution does not always guarantee a reliable evaluation. For this reason, as an integration of the methods, it is advisable to apply different analysis methods at the same time. Completeness of data and medium to long time series are prerequisites for meaningful analyses, while the use of the same time interval is necessary for comparisons between different monitoring wells and between the results of different statistical analyses.

By spatializing the results, it was possible to identify areas characterized by similar GWL behaviour. These influences vary locally in the Piedmont plain and require local assessments to determine the impact of changes in GWL.

Knowledge of current and potential future changes in GWL is important, not only because they are indicative of the total amount of water stored in an aquifer but also because they can support the choices of water management and can provide indications of the degree of exploitation of an aquifer. Understanding the mechanisms and factors that regulate GWL fluctuations and evaluating the GWL over time represent the basis for assessing the quantitative status of shallow aquifers.

However, it was seen that the application of different methods provides a clearer picture of the quantitative status of the GW resource and simultaneously highlights the need for further investigation of the recharge dynamics that should consider other climatic and anthropogenic variables as well as the local geological/geographical and climatic setting.

Future insights will analyze the effects of other natural factors (climatic, e.g., air temperature, evapotranspiration, snowmelt) and anthropogenic variables (extent of withdrawals) with an in-depth analysis of the local hydrogeological and geological characteristics of the aquifers.

The impacts of these factors on groundwater recharge are, indeed, among the most important factors to be evaluated because the variations in GWL depend on the net groundwater recharge and discharge, which relies on these parameters/factors.

CRediT authorship contribution statement

Susanna Mancini: Conceptualization, Methodology, Formal analysis, Investigation, Data curation, Visualization, Writing – original draft. **Elena Egidio:** Data curation, Writing – original draft. **Domenico Antonio De Luca:** Methodology, Writing – original draft. **Manuela Lasagna:** Conceptualization, Methodology, Formal analysis, Visualization, Writing – original draft, Supervision.

Data availability

Data will be made available on request.

Declaration of competing interest

The authors declare no conflict of interest.

Appendix A. Supplementary data

Supplementary data to this article can be found online at https://doi.org/10.1016/j.scitotenv.2022.157479.

References

Abdul Aziz, O.I., Burn, D.H., 2006. Trends and variability in the hydrological regime of the Mackenzie River basin. J. Hydrol. 319, 282–294.

Acquaotta, F., Fratianni, S., 2013. Analysis on long precipitation series in Piedmont north-West Italy. Am. J. Clim. Chang. 2, 14–24. https://doi.org/10.4236/ajcc.2013.21002.

Acquaotta, F., Fratianni, S., Terzago, S., Faletto, M., Prola, M.C., 2013. La neve sulle alpi piemontesi: quadro conoscitivo aggiornato al cinquantennio 1961–2010. Grafica Reventino Srl, 1–97. https://www.arpa.piemonte.it/pubblicazioni-2/pubblicazioni-anno-2013/arpa-neve-capp1e2.pdf.

Allocca, V., Celico, P., 2008. Scenari idrodinamici nella piana ad Oriente di napoli (Italia), nell'ultimo secolo: cause e problematiche idrogeologiche connesse. G. Geol. Appl. 9, 175–198.

Amogne, A., Simane, B., Ali Hassen, A., Bantider, A., 2018. Variability and time series trend analysis of rainfall and temperature in northcentral Ethiopia: a case study in woleka sub-basin. Weather Clim. Extremes 19, 29–41.

Apaydin, A., 2009. Response of groundwater to climate variation: fluctuations of groundwater level and well yields in the Halacli aquifer Cankiri, Turkey. Environ. Monit. Assess. 2009. https://doi.org/10.1007/s10661-009-0976-8.

Arora, M., Goel, N.K., Singh, P., 2005. Evaluation of temperature trends over India. Hydrol. Sci. J. 501, 81–93.

Asoka, A., Gleeson, T., Wada, Y., Mishra, V., 2017. Relative contribution of monsoon precipitation and pumping to changes in groundwater storage in India. Nat. Geosci. 10, 109–117.

ARPA, 2010. ARPA Piemonte. Climate and climate indicators of Piedmont. http://rsaonline.arpa.piemonte.it/meteoclima50/clima_ed_indicatori.htm. (Accessed 11 April 2021).

ARPA, 2016. ARPA Piemonte. Confronti storici – analisi lungo periodo. https://www.arpa.piemonte.it/rischinaturali/tematismi/clima/confronti-storici/analisi-lungo.html. (Accessed 11 April 2021).

ARPA, 2018. Il Clima in Piemonte nel 2017. https://www.arpa.piemonte.it/rischinaturali/tematismi/clima/rapporti-di-analisi/annuale_pdf/anno_2017.pdf. (Accessed 11 April 2021).

Baronetti, A., Acquaotta, F., Fratianni, S., 2018. Rainfall variability from a dense rain gauge network in north-West Italy. Clim. Res. 75 (3), 201–213. https://doi.org/10.3354/cr01517.

Bastiancich, L., Lasagna, M., Mancini, S., Falco, M., De Luca, D.A., 2021. Temperature and discharge variations in natural mineral water springs due to climate variability: a case study in the Piedmont Alps (NW Italy). Environ. Geochem. Health https://doi.org/10.1007/s10653-021-00864-8.

Beaulieu, C., Chen, J., Sarmiento, J.L., 2012. Change-point analysis as a tool to detect abrupt climate variations. Phil. Trans. R. Soc. A 370.

Beretta, G.P., Avanzini, M., Pagotto, A., 2004. Managing groundwater rise: experimental results and modelling of water pumping from a quarry lake in Milan urban area (Italy). Environ. Geol. 45, 600–608.

Biancotti, A., Bellardone, G., Bovo, S., Cagnazzi, B., Giacomelli, L., Marchisio, C., 1998. Distribuzione regionale di piogge e temperature. Collana Studi Climatologici in Piemonte. vol.1. Regione Piemonte, p. 80.

Birsan, M.V., Molnar, P., Burlando, P., Pfaundler, M., 2005. Streamflow trends in Switzerland. J. Hydrol. 314, 312–329.

Bove, A., Casaccio, D., Destefanis, E., De Luca, D.A., Lasagna, M., Masciocco, L., Ossella, L., Tonussi, M., 2005. Idrogeologia della pianura piemontese, Regione Piemonte. Mariogros Industrie Grafiche S.p.A, Torino.

Braca, G., Bussettini, M., Lastoria, B., Mariani, S., 2013. Anabasi – analisi stastistica di base delle serie storiche di dati idrologici – macro a supporto delle linee guida Ispra – manuale d'uso. Linee guida per l'analisi statistica di base delle serie storiche di dati idrologici. ISPRA, manuali e linee guida n.84/13, Roma, 2013 . https://www.isprambiente.gov.it/pre_meteo/idro/ANABASI_ISPRA.html. (Accessed 5 February 2022).

Burn, D.H., Elnur, H.M.A., 2002. Detection of hydrologic trend and variability. J. Hydrol. 255, 107–122.

Caloiero, T., Coscarelli, R., Ferrari, E., Mancini, M., 2011. Trend detection of annual and seasonal rainfall in Calabria southern Italy. Int. J. Climatol. 311, 44–56.

Castagna, S.E.D., De Luca, D.A., Lasagna, M., 2015. Eutrophication of Piedmont quarry lakes north-western Italy: hydrogeological factors, evaluation of trophic levels and management strategies. J. Environ. Assess. Policy Manag. 17 (4), 1550036. https://doi.org/10.1142/S1464333215500362 21 pp.

Costa, M., Gonçalves, M.P., Texeira, L., 2016. Change-point detection in environmental time series based on the informational approach. Eletron. J. Appl. Stat. Anal. 92, 267–296. https://doi.org/10.1285/i20705948v9n2p267.

Cuthbert, M.O., Acworth, R., Andersen, M., Larsen, J., McCallum, A., Rau, G.C., Tellam, J., 2015. Understanding and quantifying focused, indirect groundwater recharge from ephemeral streams using water table fluctuations.Available online at:Water Resour. Res. https://doi.org/10.1002/2015WR017503 (Accessed 24 November 2021).

De Luca, D.A., Falco, F., Falco, M., Lasagna, M., 2005. Studio della variazione del livello piezometrico della falda superficiale nella pianura vercellese (Piemonte). G. Geol. Appl. 2, 387–392.

De Luca, D.A., Lasagna, M., Debernardi, L., 2020. Hydrogeology of the western Po Plain Piedmont NW, Italy. J. Maps 16 (2), 265–273. https://doi.org/10.1080/17445647.2020.1738280.

De Luca, D.A., Lasagna, M., Mancini, S., 2019. Strategies for deep aquifers protection at local and regional scale: the Piedmont region example. GEAM Geoingegneria Ambientale e Mineraria LVI, pp. 24–29 n. 1.

Döll, P., Fiedler, K., 2008. Global-scale modeling of groundwater recharge. Hydrol. Earth Syst. Sci. 12, 863–885. https://doi.org/10.5194/hess-12-863-2008.

Döll, P., Hoffmann-Dobreva, H., Portmanna, F.T., Siebert, S., Eicker, A., Rodell, M., Strassberge, G., Scanlon, B.R., 2012. Impact of water withdrawals from groundwater and surface water on continental water storage variations. J. Geodyn. 59–60, 143–156. https://doi.org/10.1016/j.jog.2011.05.001.

Ducci, D., Polemio, M., 2018. Quantitative impact of climate variations on groundwater in southern Italy. In: Calvache, M., Duque, C., Pulido-Velazquez, D. (Eds.), Groundwater and Global Change in the Western Mediterranean Area. Environmental Earth Sciences. Springer, Cham https://doi.org/10.1007/978-3-319-69356-9_12.

EEA, 2018. European Environment Agency (EEA). European waters. Assessment of status and pressures. EEA report no 7/2018. https://www.eea.europa.eu/publications/state-of-water.

EPA, 2016. ProUCL software. Statistical software ProUCL 5.1.00 for environmental applications for data sets with and without nondetect observations. https://www.epa.gov/land-research/proucl-software. (Accessed 5 February 2022).

Fatichi, S., Ivanov, V.Yu., Caporali, E., 2012. Investigating interannual variability of precipitation at the global scale: is there a connection with Seasonality? J. Clim. 25, 5512–5523. https://doi.org/10.1175/JCLI-D-11-00356.1.

Helsel, D.R., Hirsch, R.M., Ryberg, K.R., Archfield, S.A., Gilroy, E.J., 2020. Statistical Methods in Water Resources: U.S. Geological Survey Techniques and Methods. https://doi.org/10.3133/tm4a3 book 4, chap. A3, 458 p.

Hirsch, R.M., Slack, J.R., Smith, R.A., 1982. Techniques of trend analysis for monthly water quality data. Water Resour. Res. 181, 107–121.

IAH, 2016. Global change & groundwater. Strategic overview series. https://iah.org/wp-content/uploads/2016/07/IAH-Global-Change-groundwater-14-June-2016.pdf.

IPCC, 2022. In: Pörtner, H.-O., Roberts, D.C., Tignor, M., Poloczanska, E.S., Mintenbeck, K., Alegría, A., Craig, M., Langsdorf, S., Löschke, S., Möller, V., Okem, A., Rama, B. (Eds.), Climate Change 2022: Impacts, Adaptation, and Vulnerability. Contribution of Working Group II to the Sixth Assessment Report of the Intergovernmental Panel on Climate Change. Cambridge University Press.

ISPRA, 2017. Criteri tecnici per l'analisi dello stato quantitativo e il monitoraggio dei corpi idrici sotterranei. Manuali e Linee Guida, Delibera del Consiglio SNPA del 15/05/2017-8/2017.

Kawamura, A., Bui, D.D., Tong, T.N., Nakagawa, N., Amaguchi, H., 2011. Trend Detection in Groundwater Levels of Holocene Unconfined Aquifer in Hanoi, Vietnam, by Non Parametric Approaches. https://doi.org/10.1061/4117341494.

Kendall, M.G., 1955. Rank Correlation Measures. Charles Griffin, London 202 pp.

Kiley, G., 1999. Climate change in Ireland from precipitation and streamflow observations. Adv. Water Resour. 23, 141–151.

Krishan, G., Chandniha, S.K., Lohani, A.K., 2015. Rainfall trend analysis of Punjab, India using statistical non-parametric test. Curr. World Environ. 103, 792–800. https://doi.org/10.12944/CWE.10.3.09.

Krogulec, E., Malecki, J.J., Porowoska, D., Wojdalska, A., 2020. Assessment of causes and effects of groundwater level change in an urban area Warsaw, Poland. Water 12, 3107. https://doi.org/10.3390/w12113107.

Kumar, P., Chandniha, S.K., Lohani, A.K., Krishan, G., Nema, A.K., 2018. Trend analysis of groundwater level using non-parametric tests in alluvial aquifers of Uttar Pradesh, India. Curr. World Environ. 131, 44–54. https://doi.org/10.12944/CWE.13.1.05.

Lanzante, J.R., 1996. Resistant, robust and non-parametric techniques for the analysis of climate data: theory and examples, including applications to historical radiosonde station data. Int. J. Clim. 16, 1197–1226.

Lasagna, M., Caviglia, C., De Luca, D.A., 2014. Simulation modeling for groundwater safety in an overexploitation situation: the Maggiore Valley context (Piedmont, Italy). Bull. Eng. Geol. Environ. 73, 341–355. https://doi.org/10.1007/s10064-013-0500-9.

Lasagna, M., De Luca, D.A., Franchino, E., 2018. Intrinsic groundwater vulnerability assessment: issues, comparison of different methodologies and correlation with nitrate concentrations in NW Italy. Environ. Earth Sci. 77, 277. https://doi.org/10.1007/s12665-018-7452-0.

Lasagna, M., Ducci, D., Sellerino, M., Mancini, S., De Luca, D.A., 2020a. Meteorological variability and groundwater quality: examples in different hydrogeological settings (2020). Water 12, 1297. https://doi.org/10.3390/w12051297.

Lasagna, M., Mancini, S., De Luca, D.A., Cravero, M., 2019. Piezometric levels in the Piedmont plain NW Italy: trend and hydrodynamic behaviour of the shallow aquifer. Rend. Online Soc. Geol. Ital. 48, 2–9. https://doi.org/10.3301/ROL.2019.30.

Lasagna, M., Mancini, S., De Luca, D.A., 2020b. Groundwater hydrodynamic behaviours based on water table levels to identify natural and anthropic controlling factors in the Piedmont Plain Italy. Sci. Total Environ. 716, 137051. https://doi.org/10.1016/j.scitotenv.2020.137051.

Liu, J., Cao, G., Zeng, C., 2011. Sustainability of Groundwater Resources in the North China Plain, Sustaining Groundwater Resources: A Critical Element in the Global Water Crisis, pp. 69–87 https://doi.org/10.1007/978-90-481-3426-7_5.

Lockwood, J.G., 2001. Abrupt and sudden climatic transitions and fluctuations: a review. Int. J. Climatol. 21 (9), 1153–1179. https://doi.org/10.1002/joc.630.

Lutz, A., Minyila, S., Saga, B., Diarra, S., Apambire, B., Thomas, J., 2015. Fluctuation of groundwater levels and recharge patterns in Northern Ghana. Climate 3, 1–15. https://doi.org/10.3390/cli3010001.

Mann, H.B., 1945. Nonparametric tests against trend. Econometrica 13, 245–259.

Mariani, L., 2006. Alcuni metodi per l'analisi delle serie storiche in agrometeorologia. Rivista Italiana di Agrometeorologia 56 (2), 48.

MOE (Ministry od Environment), 2008. Guidance Document for Using the Percentile Method for Calculating Trigger Levels for Groundwater for the Ontario Low Water Response Plan. Ministry of Environment March 2008.

Ng, G.-H.C., McLaughlin, D., Entekhabi, D., Scanlon, B.R., 2010. Probabilistic analysis of the effects of climate change on groundwater recharge. Water Resour. Res. 46, W07502. https://doi.org/10.1029/2009WR007904.

Panda, D.K., Mishra, A., Jena, S.K., James, B.K., Kumar, A., 2007. The influence of drought and anthropogenic effects on groundwater levels in Orissa, India. J. Hydrol. 3433, 140–153. https://doi.org/10.1016/j.jhydr ol.2007.06.007.

Panda, D., Mishra, A., Kumar, A., 2012. Quantification of trends in groundwater levels of Gujarat in western India. Hydrol. Sci. J. 57, 1325–1336.

Pathak, A.A., Dodamani, B.M., 2019. Trend analysis of groundwater levels and assessment of regional groundwater drought: Ghataprabha River Basin, India. Nat. Resour. Res. 28, 631. https://doi.org/10.1007/s11053-018-9417-0.

Patle, G.T., Singh, D.K., Sarangi, A., Anil, R., Khanna, M., Sahoo, R.N., 2015. Time series analysis of groundwater levels and projection of future trend. J. Geol. Soc. India 852, 232–242.

Perotti, L., Carraro, G., Giardino, M., De Luca, D.A., Lasagna, M., 2019. Geodiversity evaluation and water resources in the Sesia Val Grande UNESCO Geopark (Italy). Water 2019 (11), 2102. https://doi.org/10.3390/w11102102.

Pettitt, N., 1979. A non parametric approach to the change-point problem. Appl. Stat. 28 (2).

Polemio, M., Casarano, D., 2008. Climate change, drought and groundwater availability in southern Italy. In: Dragoni, W., Sukhija, B.S. (Eds.), Climate Change and Groundwater. 288. The Geological Society Special Publications, pp. 39–51. https://doi.org/10.1144/SP288.4.

Polemio, M., 2016. Monitoring and management of Karstic coastal groundwater in a changing environment Southern Italy: a review of a regional experience. Water 84, 1–16.

Post, R., 2013. Percentile groundwater indicator literature review. Nottawasaga Valley Conservation Authority 8195 8th Line, Utopia, ON, L0M 1T0 705-424-1479.

Rai, S.N., Singh, R.N., 1985. Water table fluctuations in response to time varying recharge. In: Diskin, M. (Ed.), Scientific Basis for Water Resources Management. 153. IAHS Publ. No, pp. 287–294.

Reeves, J., Chen, J., Wang, X.L., Lund, R., Lu, Q.Q., 2007. A review and comparison of changepoint detection techniques for climate data. J. Appl. Meteorol. Climatol. 466, 900–915.

Regione Piemonte, 2020. Report 2020 – Analisi clima regionale periodo 1981- 2010 e tendenze negli ultimi 60 anni. https://www.regione.piemonte.it/web/sites/default/files/media/documenti/2021-02/analisi_clima_regionale_1981-2010.pdf. (Accessed 11 April 2021).

Regione Piemonte, 2021a. Idrogeologia – Carta dei complessi idrogeologici. https://www.geoportale.piemonte.it/geonetwork/srv/ita/catalog.search#/metadata/r_piemon:6e15300b-d6f1-45a2-a82c-08e2541b1981.

Regione Piemonte, 2021b. http://www.regione.piemonte.it/monitgis/jsp/cartografia/mappa.do. (Accessed 11 April 2021).

Regione Piemonte, 2021c. RAM - Banca dati agrometereologica | Servizionline. https://servizi.regione.piemonte.it/catalogo/ram-banca-dati-agrometereologica. (Accessed 11 April 2021).

Ribeiro, L., Kretschmer, N., Nascimento, J., Buxo, A., Rötting, T., Soto, G., Señoret, M., Oyarzún, J., Maturana, H., Oyarzún, R., 2015. Evaluating piezometric trends using the MannKendall test on the alluvial aquifers of the Elqui River basin, Chile. Hydrol. Sci. J. 60 (10), 1840–1852. https://doi.org/10.1080/02626667.2014.945936.

Rusi, S., Chiaudani, A., Palmucci, W., Di Lena, B., 2013. Fluctuations and trends of piezometric levels: a case study in Abruzzo. Convegno AIAM.

Russo, T.A., Lall, U., 2017. Depletion and response of deep groundwater to climate-induced pumping variability. Nat. Geosci. 2017 (10), 105–108.

Sen, P.K., 1968. Estimates of the regression coefficient based on Kendall's tau. J. Am. Stat. Assoc. 63, 1379–1389.

Serrano, A., Mateos, V.L., Garcia, J.A., 1999. Trend analysis of monthly precipitation over the Iberian Peninsula for the Period 1921–1995. Phys. Chem. Earth 241–2, 85–90.

Soliani, L., 2001. Fondamenti di statistica applicata all'analisi e alla gestione dell'ambiente. Libreria medico scientifica, Parma 1139pp.

Stahl, K., Hisdal, H., Hannaford, J., Tallaksen, L.M., van Lanen, H.A.J., Sauquet, E., Demuth, S., Fendekova, M., Jodar, J., 2010. Streamflow trends in Europe: evidence from a dataset of near-natural catchments. Hydrol. Earth Syst. Sci. Discuss. 7, 5769–5804.

Svensson, C., Kundzewicz, W.Z., Maurer, T., 2005. Trend detection in river flow series: 2. Flood and low-flow index series. Hydrol. Sci. J. 50, 5.

Tabari, H., Nikbakht, J., Some'e, B.S., 2011. Investigation of groundwater level fluctuations in the north of Iran. Environ. Earth Sci. 661, 231–243.

Taylor, R.G., Scanlon, B., Döll, P., Rodell, M., Beek, R.V., Wada, Y., Longuevergne, L., Leblanc, M., Famiglietti, J., Edmunds, M., et al., 2013. Ground water and climate change. Nat. Clim. Chang. 2012 (3), 322–329. https://doi.org/10.1038/nclimate1744.

Tirogo, J., Jost, A., Biaou, A., Valdes-Lao, D., Koussoubé, Y., Ribstein, P., 2016. 2016 climate variability and groundwater response: a case study in Burkina Faso West Africa. Water 8, 171. https://doi.org/10.3390/w8050171.

Tomé, A.R., Miranda, P.M.A., 2004. Piecewise linear fitting and trend changing points of climate parameters. Geophys. Res. Lett. 31, L02207.

Tomozeiu, R., Busuioc, A., Marletto, V., Zinotti, F., Cacciamani, C., 2000. Detection of changes in the summer precipitation time series of the region Emilia-Romagna, Italy. Theor. Appl. Climatol. 67, 193–200.

Toreti, A., Desiato, F., Fioravanti, G., Perconti, W., 2010. Seasonal temperatures over Italy and their relationship with low frequency atmospheric circulation patterns. J. Clim. Chang. 99, 211–227.

Voss, K.A., Famiglietti, J.S., Lo, M., Linage, C., Rodell, M., Swenson, S.C., 2013. Groundwater depletion in the Middle East from GRACE with implications for transboundary water management in the Tigris-Euphrates-Western Iran region. Water Resour. Res. 49. https://doi.org/10.1002/wrcr.20078.

Wada, J., van Beek, L.P.H., van Kempten, C., Reckman, J.W.T.M., Vasak, S., Bierkens, M.P.F., 2010. Global depletion of groundwater resources. Geophys. Res. Lett. 37, l20402. https://doi.org/10.1029/2010GL044571.

Whittemore, D.O., Butler, J.J., Wilson, B.B., 2016. Assessing the major drivers of water-level declines: new insights into the future of heavily stressed aquifers. Hydrol. Sci. J. 61, 134–145.

WMO, 2007. The Role of Climatological Normals in a Changing Climate WMO/TD-No. 1377. 9. Worldwide. Hydrol. Current Res, Geneva , p. 303. https://library.wmo.int/index.php?lvl=notice_display&id=16659#.YnahP-hBxPY.

WMO, 2017. Guidelines on the calculation of climate normals WMO- No. 1203. https://library.wmo.int/index.php?lvl=notice_display&id=20130#.YnT2UtpBxPY.

Wu, W.J., Lo, M.H., Wada, J., Famiglietti, J.S., Reager, J.T., Yeh, P.J.F., Ducharne, A., Yang, Z.L., 2020. Divergent effects of climate change on future groundwater availability in key mid-latitude aquifers. Nat. Commun. 11, 3710. https://doi.org/10.1038/s41467-020-17581-y.

Xia, J., Wu, X., Zhan, C., Qiao, Y., Hong, S., Yang, P., Zou, L., 2019. Evaluating the dynamics of groundwater depletion for an arid land in the Tarim Basin. China Water 11, 186. https://doi.org/10.3390/w11020186.

Xiong, L., Guo, S., 1994. Trend test and change-point detection for the annual discharge series of the Yangtze River at the Yichang hydrological station. Hydrol. Sci. J. 49 (1), 99–112. https://doi.org/10.1623/hysj.49.1.99.53998.

Xu, K., Milliman, J.D., Xu, H., 2010. Temporal trend of precipitation and runoff in major Chinese Rivers since 1951. Glob. Planet. Chang. 73 (3–4), 219–232. https://doi.org/10.1016/j.gloplacha.2010.07.002.

Zhang, X., Harvey, K.D., Hogg, W.D., Yuzyk, T.R., 2001. Trends in Canadian streamflow. Water Resour. Res. 374, 987–998. https://doi.org/10.1029/2000WR900357.

Zheng, C., Liu, J., Cao, G., Kendy, E., Wang, H., Jia, Y., 2010. Can China cope with its water crisis? – Perspectives from the North China Plain. Groundwater 48 (3), 350–354.

Zwilling, D., Leete, J., Rongitsch, B., 1989. Understanding Groundwater Level Trend: A Key to Managing Water Use. Division of water, Minnesota department of natural resources.